Title

Genetic architecture of the acute and persistent immune cell response after radiation exposure.

Journal

Cell Genomics, 3(11)

Authors

Snijders, Antoine

He, Li

Zhong, Chenhan

et al.

Publication Date

2023-11-08

DOI

10.1016/j.xgen.2023.100422

Peer reviewed

Cell Genomics

Resource

Genetic architecture of the acute and persistent immune cell response after radiation exposure

Graphical abstract

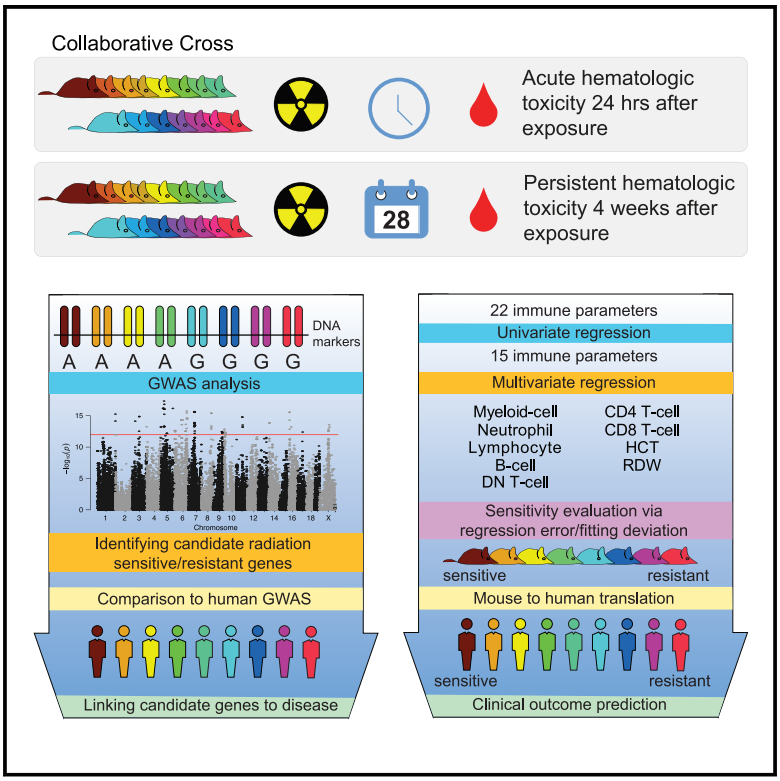

Highlights

- Hematologic toxicity after radiation exposure varies widely across individuals
- GWAS analyses identified many new radiation sensitivity genes
- A radiation sensitivity score was developed in a population-based mouse model
- The murine radiation sensitivity score predicts outcome in cancer patients

Authors

Li He, Chenhan Zhong, Hang Chang, ..., Scott C. Kogan, Jian-Hua Mao, Antoine M. Snijders

Correspondence

jhmao@lbl.gov (J.-H.M.), amsnijders@lbl.gov (A.M.S.)

In brief

He et al. present a community resource of immune parameters and genome-wide association analyses at baseline and after radiation exposure for investigations of contributions of host genetics on radiosensitivity. Genome-wide association analysis identified many new genes associated with radiation sensitivity. A mouse-to-human translation revealed the predictive value of a radiation resistance score for relapse-free survival in a cohort of medulloblastoma patients.

He et al., 2023, Cell Genomics *3*, 100422
November 8, 2023
https://doi.org/10.1016/j.xgen.2023.100422

CellPress

Cell Genomics

CellPress
OPEN ACCESS

Resource

Genetic architecture of the acute and persistent immune cell response after radiation exposure

Li He,[1,2,11] Chenhan Zhong,[2,3,11] Hang Chang,[2,4,11] Jamie L. Inman,[2,4,11] Susan E. Celniker,[2,10] Myrsini Ioakeim-Ioannidou,[5] Kevin X. Liu,[6] Daphne Haas-Kogan,[6] Shannon M. MacDonald,[5] David W. Threadgill,[7,8] Scott C. Kogan,[9] Jian-Hua Mao,[2,4,10,*] and Antoine M. Snijders[2,4,10,12,*]

[1]Department of Hematology, Zhongnan Hospital, Wuhan University, Wuhan, Hubei 430079, China
[2]Biological Systems and Engineering Division, Lawrence Berkeley National Laboratory, Berkeley, CA 94720, USA
[3]Department of Medical Oncology, Key Laboratory of Cancer Prevention and Intervention, Ministry of Education, The Second Affiliated Hospital, Zhejiang University School of Medicine, Hangzhou, Zhejiang 310009, China
[4]Berkeley Biomedical Data Science Center, Lawrence Berkeley National Laboratory, Berkeley, CA 94720, USA
[5]Department of Radiation Oncology, Massachusetts General Hospital, Boston, MA 02114, USA
[6]Department of Radiation Oncology, Brigham and Women's Hospital, Dana-Farber Cancer Institute, Boston Children's Hospital, Harvard Medical School, Boston, MA 02115, USA
[7]Texas A&M Institute for Genome Sciences and Society, Texas A&M University, College Station, TX 77843, USA
[8]Departments of Nutrition and Cell Biology and Genetics, Texas A&M University, College Station, TX 77843, USA
[9]Department of Laboratory Medicine, University of California, San Francisco, San Francisco, CA 94143, USA
[10]Comparative Biochemistry Program, University of California Berkeley, Berkeley, CA 94720, USA
[11]These authors contributed equally
[12]Lead contact
*Correspondence: jhmao@lbl.gov (J.-H.M.), amsnijders@lbl.gov (A.M.S.)
https://doi.org/10.1016/j.xgen.2023.100422

SUMMARY

Hematologic toxicity is a common side effect of multimodal cancer therapy. Nearly all animal studies investigating the causes of radiotherapy-induced hematologic toxicity use inbred strains with limited genetic diversity and do not reflect the diverse responses observed in humans. We used the population-based Collaborative Cross (CC) mouse resource to investigate the genetic architecture of the acute and persistent immune response after radiation exposure by measuring 22 immune parameters in 1,720 CC mice representing 35 strains. We determined relative acute and persistent radiation resistance scores at the individual strain level considering contributions from all immune parameters. Genome-wide association analysis identified quantitative trait loci associated with baseline and radiation responses. A cross-species radiation resistance score predicted recurrence-free survival in medulloblastoma patients. We present a community resource of immune parameters and genome-wide association analyses before and after radiation exposure for future investigations of the contributions of host genetics on radiosensitivity.

INTRODUCTION

Radiotherapy is a component of cancer treatment for more than half of all cancer patients.[1] Improvements in radiotherapy technology over the past decades have led to improved precision of radiation delivery to target volumes, allowing higher doses to be delivered to the tumor while at the same time minimizing the dose delivered to normal surrounding tissues. Given the sensitivity of lymphocytes to radiation exposure, radiation injury to the hematopoietic system is a common side effect of radiotherapy. Injury to the hematopoietic system can be acute or chronic because of effects on blood-forming organs such as the bone marrow. Radiation-induced depletion of circulating lymphocyte populations has been associated with reduced overall survival in a variety of solid cancer types,[2–6] suggesting that the immune system plays an important role in improving the efficacy of radiation therapy. The human immune system functions to fight disease and consists of a complex network of cells, tissues, and organs, which closely work together in maintaining optimal health. Abundance levels of lymphocyte populations are tightly regulated, balancing cell proliferation and programmed cell death, to maintain immune cell homeostasis. Genetic variants are well known to influence the immune system and immune responses to radiation exposure. Furthering our understanding of individual sensitivity to radiation-induced hematopoietic injury could assist in identifying biomarkers that can predict injury. Moreover, identifying novel targets for therapeutic intervention could prevent hematopoietic injury and further increase patient survival after radiotherapy.

The discovery of genes associated with hematopoietic radiation sensitivity can be facilitated by the experimental use of genetic reference populations with known genomes to dissect the complex interactions. Furthermore, such an approach may

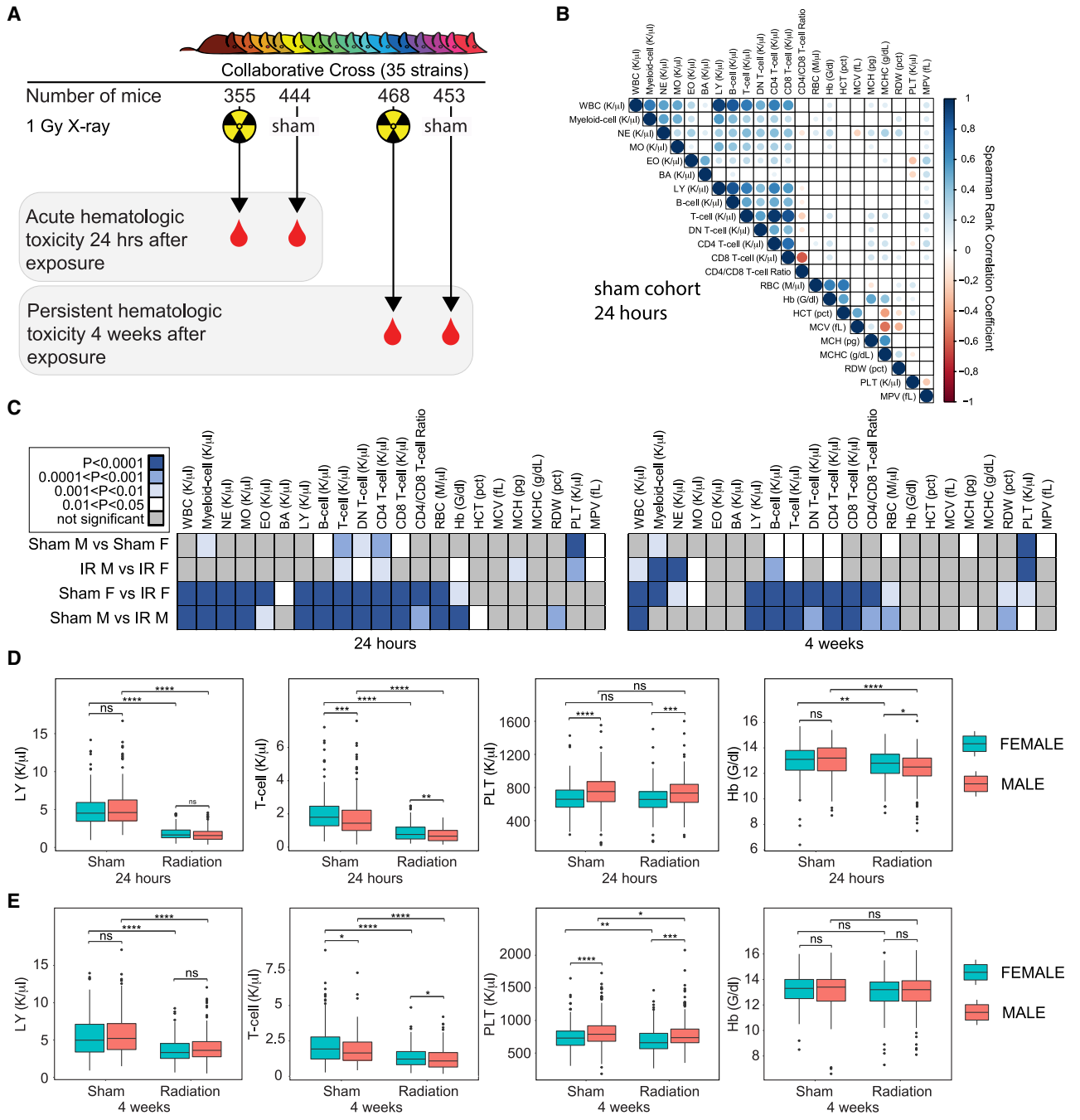

Figure 1. Hematologic toxicity in Collaborative Cross mice

(A) Schematic diagram of experimental design. Different strains of the CC resource were irradiated whole body with 1 Gy of X-rays or not irradiated in the control group. 24 h or 4 weeks after radiation exposure, blood was collected for complete blood count analysis from treated and control animals.

(B) Spearman's rank correlation analyses of 22 hematologic parameters in unirradiated mice (24-h cohort) across different CC strains. Positive and negative correlations are indicated in blue and red, respectively, and further clarified by circle size.

(C) Population-level comparisons of hematologic parameters between male and female mice across all CC strains at 24 h (left) and 4 weeks (right) after radiation or sham exposure. Non-significant comparisons are indicated in gray, whereas significant comparisons are indicated in white ($0.01 < p < 0.05$) or different shades of blue ($p < 0.01$).

(D) Comparison of different hematologic parameters between irradiated and sham irradiated female (blue) and male (red) mice at 24 h after exposure.

(legend continued on next page)

ultimately provide insight into immune-related diseases by identifying potential underlying molecular mechanisms. The natural genetic variation in population-based mouse models offers unprecedented opportunities to identify the primary genetic loci that drive susceptibility to specific environmental exposures and to investigate their mechanistic contributions. We have carried out comprehensive immunophenotyping after radiation exposure in the Collaborative Cross (CC), a large multi-parental panel of recombinant inbred strains. The CC is a population of mice that contains a level of genetic and phenotypic diversity on par with the human population.[7] These studies provide a community resource of radiation sensitivity using 22 individual immune parameters, including genetic mapping of baseline (unirradiated) and irradiated cohorts at 24 h and 4 weeks after radiation exposure. Our study developed a novel analysis pipeline for determining radiation resistance scores and identified 22 and 5 genetic loci that govern the mammalian radiation response at 24 h and 4 weeks after exposure, respectively. Using transfer learning, we used the acute radiation sensitivity immune model in CC mice to assign a radiation resistance score to individual medulloblastoma patients and found the score to predict relapse-free survival.

RESULTS

Radiation-induced hematologic toxicity varies widely in medulloblastoma patients

We first explored the variability in hematologic effects of craniospinal irradiation in a cohort of pediatric patients with medulloblastoma using photon or proton therapy. A comprehensive complete blood count was measured in 99 patients (age range at diagnosis: 3–22 years) with newly diagnosed medulloblastoma before and 1 week after the first week of craniospinal radiation to study the acute radiation response. 1 week after the first radiotherapy treatment, we observed a significant decrease in most immune parameters, including white blood cell (WBC) counts (Table S1). For example, before the first radiotherapy fraction, the median absolute lymphocyte count was 1.94 (range 0.41–7.35) K/μL. One week after the first week of radiation treatment, median absolute lymphocyte counts significantly decreased to 0.74 K/μL (range 0.14–2.89 K/μL; $p = 3.8E{-}14$). To determine the extent of variability in radiation sensitivity across the patient cohort, we calculated for each patient the ratio of absolute lymphocyte and neutrophil counts before and after the first radiotherapy fraction. Across the cohort, the ratios ranged from 0.08 to 1.80 and from 0.07 to 2.06 for lymphocytes and neutrophils, respectively (Figure S1). We conclude that the hematologic effects of radiotherapy vary widely across individuals. We hypothesize that host genetics is an important factor in determining the level of injury to the hematopoietic system after radiotherapy, as well as the response of the hematopoietic system following injury.

Population-based radiation-induced hematologic toxicity

We then explored the influence of host genetics on the immunophenotype and radiation response in 1,720 CC mice representing 35 individual strains (Figure 1A; Table S2). Immunophenotyping included a comprehensive 22-parameter complete blood count, including the absolute abundance of specific immune cell populations including B cells, T cells, $CD4^+$ T cells, and $CD8^+$ T cells using flow cytometry. Mice were exposed at 12 weeks of age to 1 Gy whole-body X-ray radiation or sham irradiated, and blood was collected at 24 h after radiation exposure (444 sham and 355 exposed) or, in a separate cohort of mice, 4 weeks after radiation exposure (453 sham and 468 exposed). At the population level, in the unirradiated 24-h cohort, we observed strong positive correlations among WBC parameters and among erythrocyte parameters (Figure 1B). For example, hematocrit (HCT) and mean corpuscular volume (MCV) parameters were negatively correlated with mean corpuscular hemoglobin (MCH) concentration (MCHC; Spearman's rank correlation coefficient < -0.4). These correlations were largely similar 24 h after 1 Gy X-ray exposure (Figure S2A); a new negative correlation between B cell counts and the ratio of $CD4^+/CD8^+$ T cells (Spearman's rank correlation coefficient = −0.41; $p = 4.44E{-}16$) was observed 24 h after radiation exposure. Similar results were obtained in the cohort of mice analyzed 4 weeks after sham or 1 Gy irradiation (Figures S2B and S2C).

We next investigated sex differences in immune parameters between sham and irradiated mouse cohorts at 24 h and 4 weeks after radiation exposure. At 24 h after exposure, significant differences in sham irradiated male and female mice were observed for myeloid counts, B cells, T cell fractions (including double-negative [DN], $CD4^+$, and $CD8^+$ T cells), platelets (PLTs), and mean PLT volume (MPV; $p < 0.05$; Figures 1C and 1D; Data S1). Sex differences in T cell fractions (including DN and $CD4^+$ T cells), PLTs, and MPV were also observed after radiation exposure ($p < 0.05$; Figures 1C and 1D; Data S1). At the population level, T cell counts were lower in male mice compared with female mice, and this difference was maintained after radiation exposure ($p < 0.01$; Figure 1D). The radiation response at 24 h after exposure was similar between male and female mice, with 14 of 22 parameters significantly reduced after radiation exposure in both male and female mice ($p < 0.05$; Figure 1C). Four weeks after radiation exposure, the lymphocyte fractions remained significantly reduced in both male and female mice (Figures 1C and 1E; Data S2). Interestingly, the myeloid, neutrophil, and monocyte counts were significantly different between male and female mice 4 weeks after radiation exposure. In female mice, counts remained significantly lower in irradiated mice compared with sham ($p < 0.05$), whereas levels were not significantly different between sham and irradiated male mice (Figure 1C; Data S2). PLT levels were significantly higher in male mice compared with female mice in both the 24-h and 4-week cohorts

(E) Comparison of different hematologic parameters between irradiated and sham irradiated female (blue) and male (red) mice at 4 weeks after exposure. Box and whisker plots indicate median, 25th and 75th percentiles, 5th and 95th percentiles, and individual samples beyond these limits. Outliers are cases with values beyond 1.5 times the interquartile range.
The p values were obtained using the Mann-Whitney test: *$p < 0.05$, **$p < 0.01$, ***$p < 0.001$, ****$p < 0.0001$. ns, not significant.

($p < 0.001$). Interestingly, PLT levels were not affected by radiation exposure at 24 h (Figure 1D) but were significantly reduced 4 weeks after radiation exposure in both male and female mice ($p < 0.05$; Figures 1D and 1E; Data S1 and S2). We conclude that, at the population level, whole-body exposure to 1 Gy X-rays significantly affected immune parameters 24 h after exposure, and that most lymphocyte parameters remained affected in the majority of strains 4 weeks after exposure.

Strain-level differences in radiation-induced hematologic toxicity

In unirradiated and irradiated mice, the relative abundance of specific immune parameters and cell populations was tightly constrained within each strain but varied across different strains (Data S3 and S4). For subsequent analyses, strains were excluded if either the sham or irradiated cohorts contained less than three mice, leaving 33 and 31 CC strains for the 24-h and 4-week cohorts, respectively. For each immune parameter across CC strains, we calculated the ratio of the levels after irradiation over the median level in sham irradiated mice. At 24 h after radiation exposure, all CC strains exhibited a significant decrease in WBC, lymphocyte, and B cell counts, although the magnitude of the depletion varied considerably across strains (Figure 2A; Data S3). The $CD4^+/CD8^+$ T cell ratio significantly increased in 16 of 33 strains, consistent with prior reports that $CD8^+$ T cells are more sensitive to radiation exposure compared with $CD4^+$ T cells (Figure 2A).[8] To determine relative radiation sensitivity at the individual strain level based on all immune parameters, we established a pipeline combining univariate and multivariate regression analysis with regression error fitting deviation analysis (Figure 2B). First, using all 22 immune parameters, we used a univariate regression analysis to determine which phenotypes were significantly associated with radiation exposure. At 24 h after radiation, this resulted in 15 phenotypes being selected, which were subsequently down-selected using multivariate regression analysis to nine individual immune parameters, including myeloid counts, neutrophil counts, B cells, DN T cells, $CD4^+$ T cells, $CD8^+$ T cells, HCT, and red cell distribution width (RDW) (Figure 2B). Based on these nine immune parameters, we performed radiation sensitivity evaluation and assigned a radiation resistance score to each CC strain via regression error fitting deviation analysis using 10,000 bootstrapping iterations and a sampling rate of 60% (Figure 2C). Significant variation in radiation resistance at 24 h after radiation exposure was observed across CC strains ranging from 0.00076 for CC024 to 0.56 for CC002. Based on the score, we stratified CC strains into cohorts including radiation sensitive (n = 11), intermediate (n = 11), and resistant (n = 11) (Figure 2C).

At 4 weeks after radiation exposure, fewer immune parameters were significantly different between irradiated and sham irradiated mice, indicating significant recovery in immune parameters. However, WBC counts remained significantly lower compared with age-matched controls for 18 of 31 CC strains (Figure 3A). Complete recovery of lymphocyte, B cell, and T cell counts (including CD4/CD8 negative [DN], $CD4^+$, and $CD8^+$ T cells) was observed in four strains (CC011, CC026, CC030, and CC040; Figure 3A; Data S4). Similar to the radiation sensitivity evaluation at 24 h, we analyzed the data at 4 weeks to assign a radiation resistance score to each CC strain. After univariate regression analysis, we selected 12 of 22 phenotypes significantly associated with radiation exposure, which were subsequently down-selected using multivariate regression analysis to seven individual immune parameters, including myeloid counts, lymphocyte counts, $CD8^+$ T cells, $CD4^+/CD8^+$ T cell ratio, MCV, MCH, and RDW (Figure 3B). A radiation resistance score was calculated for each CC strain via regression error fitting deviation analysis (Figure 3C). Significant variation in radiation resistance at 4 weeks after radiation exposure was observed across CC strains ranging from 0.071 for CC024 to 0.498 for CC033. We stratified CC strains into three cohorts, including radiation sensitive (n = 10), intermediate (n = 11), and resistant (n = 10) (Figure 3C), and compared the radiation sensitivity assignment at 24 h with the assignment in the 4-week cohort. We observed three groups (Figure 3D). The first group included strains that were assigned the same sensitivity index at 24 h and at 4 weeks after radiation exposure. The second group included strains that were assigned an intermediate or sensitive index at 24 h and an improved index at 4 weeks after radiation exposure. The third group included strains that were assigned an intermediate or resistant index at 24 h and a more sensitive index at 4 weeks after radiation exposure. These data suggest that early hematologic effects of radiation exposure have limited power to predict longer-term recovery.

To determine the effect of sex on strain-level differences in radiation-induced hematologic toxicity, we split the cohort by sex and then, using all 22 immune parameters, determined strain-level radiation sensitivity at 24 h and 4 weeks after exposure (Figure S3). At 24 h, after univariate and multivariate regression analysis, six parameters were selected in male mice (lymphocyte counts, B cell, T cell, DN T cell, $CD4^+$ T cell, and the $CD4^+/CD8^+$ T cell ratio) and female mice (WBC, neutrophil, B cell, T cell, $CD8^+$ T cell, and red blood cell [RBC]) (Figure S3A). Based on these immune parameters, we performed radiation sensitivity evaluation for male and female mice separately and assigned a radiation resistance score to each CC strain via regression error fitting deviation. We then compared the radiation sensitivity ranking of male and female mice for each CC strain with the ranking in the sex-combined cohort (Figure S3A). Spearman's rank correlation analyses showed significant correlations between male mice and the combined cohort (Rho = 0.86; p = 1.52E−07) and female mice and the combined cohort (Rho = 0.75; p = 1.75E−06). At 4 weeks after exposure, sex-separated univariate and multivariate analyses selected seven phenotypes in male mice (WBC, lymphocyte counts, $CD4^+$ T cell, $CD8^+$ T cell, $CD4^+/CD8^+$ T cell ratio, MCH, and MCV) and nine phenotypes in female mice (lymphocyte counts, myeloid counts, $CD8^+$ T cell, $CD4^+/CD8^+$ T cell ratio, RBC, HCT, MCH, RDW, and PLT) (Figure S3B). Compared with the sex-combined cohort, the radiation sensitivity ranking of the female mice was significantly correlated with the sex-combined cohort ranking (Spearman's rank Rho = 0.81; p = 8.5E−07), whereas the radiation sensitivity ranking of the male mice did not significantly correlate with the combined cohort (Spearman's rank Rho = 0.34; p = 0.06) (Figure S3B). Together, these data suggest that sex does not influence acute hematologic radiation sensitivity but could influence longer-term recovery of the hematopoietic system.

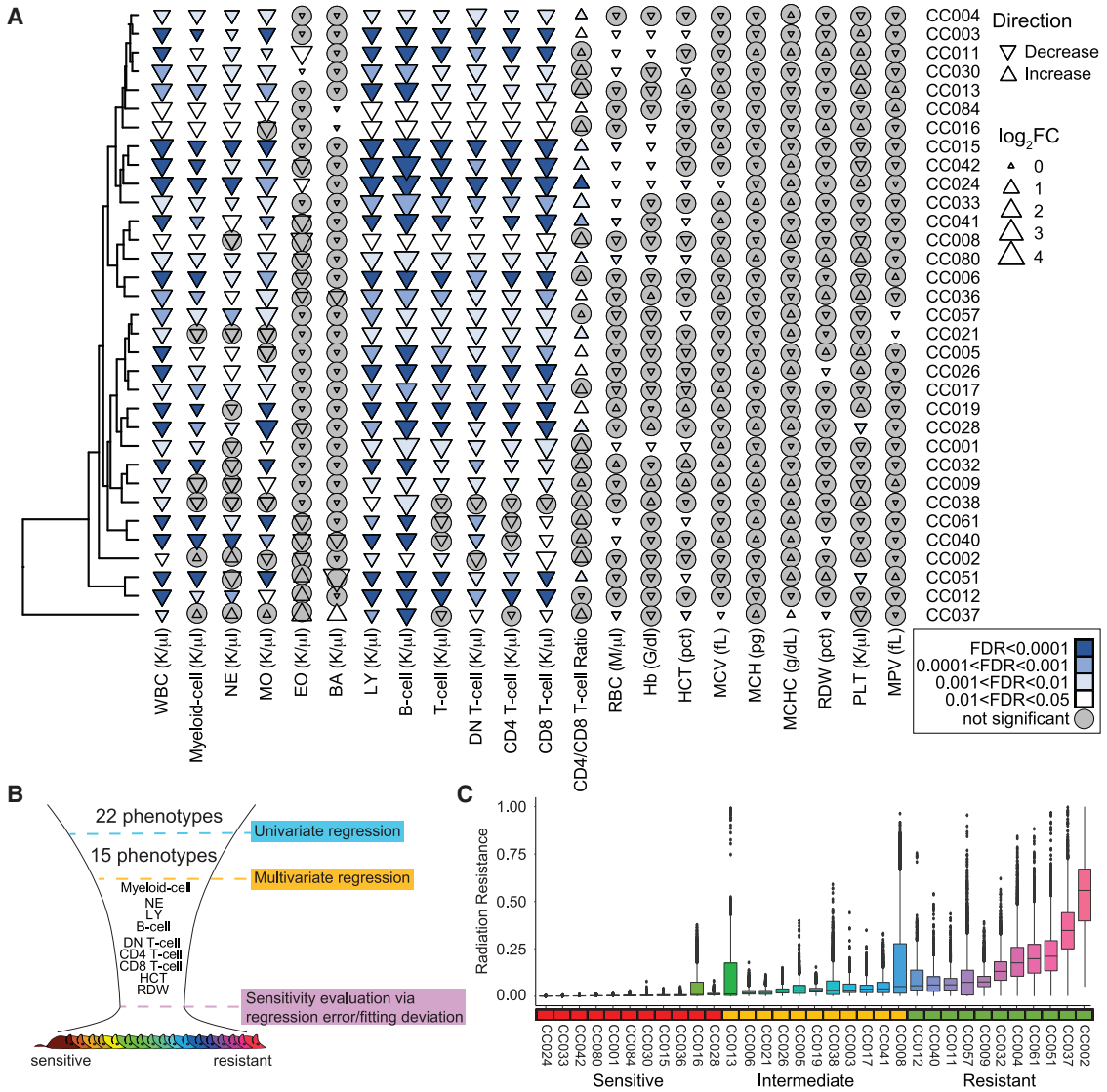

Figure 2. Radiation sensitivity 24 h after radiation exposure

(A) Hierarchical clustering of 33 CC strains based on the fold change of 22 hematologic parameters (increased: △; decreased: ▽) between irradiated and sham irradiated mice 24 h after radiation exposure. Comparisons that were not significant are indicated with a gray circle. Significant comparisons are indicated in white ($0.01 < p < 0.05$) or different shades of blue ($p < 0.01$). The p values shown were obtained using the Mann-Whitney test.

(B) Hematologic radiation sensitivity and resistance were determined by univariate and multivariate analyses followed by sensitivity evaluation via regression error/fitting deviation.

(C) Radiation resistance score for all 33 CC strains based on nine hematologic parameters. Box and whisker plots indicate median, 25th and 75th percentiles, 5th and 95th percentiles, and individual samples beyond these limits. Outliers are cases with values beyond 1.5 times the interquartile range. CC strains were divided into tertiles based on radiation sensitivity.

To determine the effect of radiation exposure on bone marrow apoptosis and reconstitution capacity, we selected CC019 and CC042, strains with differing radiation sensitivities: CC019 was assigned intermediate at 24 h and sensitive at 4 weeks after radiation exposure, whereas CC042 was assigned sensitive at 24 h and resistant at 4 weeks. Bone marrow was collected from femurs of three groups of two mice for each strain after sham and 1 Gy X-ray exposure at 24 h and 4 weeks after radiation exposure. Apoptosis, determined by the percentage of terminal deoxynucleotidyl transferase dUTP nick-end labeling (TUNEL)-positive cells, was significantly increased in bone marrow at 24 h in both CC019 ($p = 0.018$) and CC042 ($p = 8.95E-05$) (Figure 4A). No significant difference in apoptosis was observed in either strain at 4 weeks after radiation exposure. We then investigated the proliferation and differentiation ability of hematopoietic stem and progenitor cells using the colony-forming unit (CFU) assay. Bone marrow stem cells were isolated, plated in triplicate and hematopoietic colonies, including total

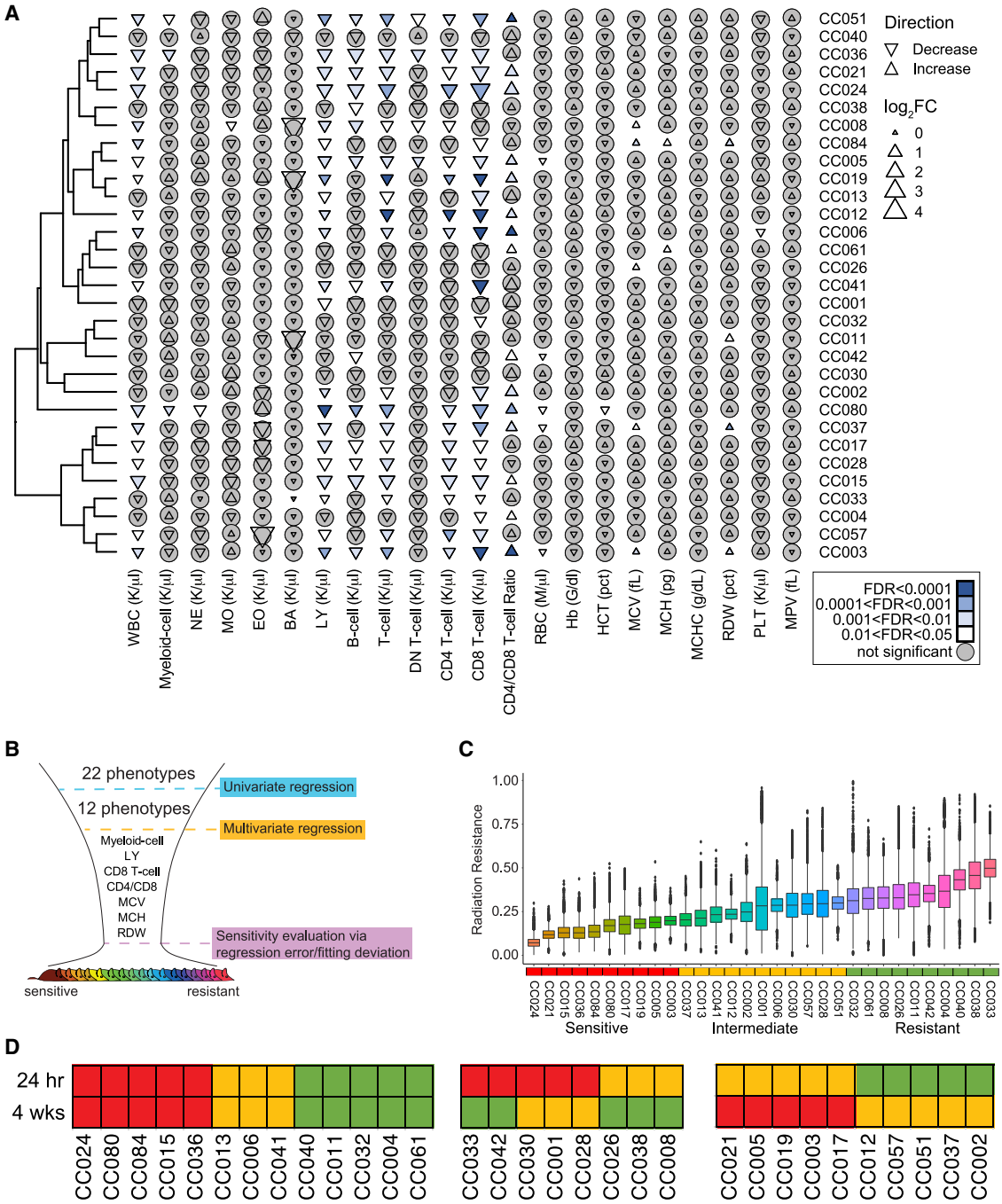

Figure 3. Radiation sensitivity 4 weeks after radiation exposure

(A) Hierarchical clustering of 31 CC strains based on the fold change of 22 hematologic parameters (increased: △; decreased: ▽) between irradiated and sham irradiated mice 4 weeks after radiation exposure. Comparisons that were not significant are indicated with a gray circle. Significant comparisons are indicated in white ($0.01 < p < 0.05$) or different shades of blue ($p < 0.01$). The p values shown were obtained using the Mann-Whitney test.

(B) Hematologic radiation sensitivity and resistance were determined by univariate and multivariate analyses followed by sensitivity evaluation via regression error/fitting deviation.

(C) Radiation resistance score for all 31 CC strains based on seven hematologic parameters. Box and whisker plots indicate median, 25th and 75th percentiles, 5th and 95th percentiles, and individual samples beyond these limits. Outliers are cases with values beyond 1.5 times the interquartile range. CC strains were divided into tertiles based on radiation sensitivity.

(D) Three groups were observed: the first group maintained the same sensitivity index (red = sensitive, yellow = intermediate, green = resistant) at 24 h and at 4 weeks (13 strains), the second group went from intermediate or sensitive at 24 h to an improved score at 4 weeks (8 strains), and the third group was assigned intermediate or resistant at 24 h and a more sensitive index at 4 weeks (10 strains).

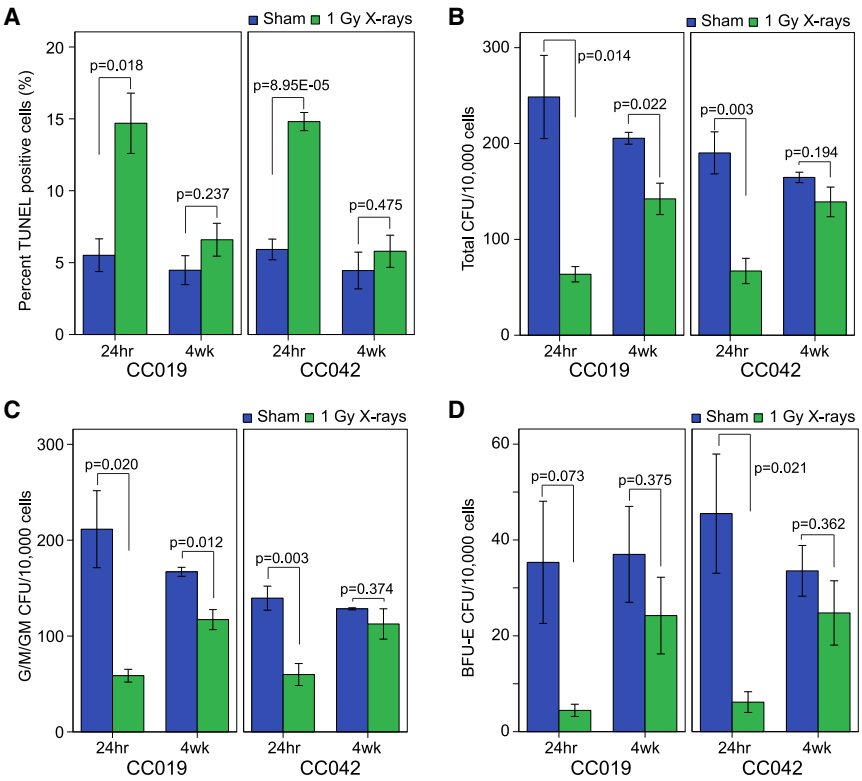

Figure 4. Assessment of effect of genetic background on radiation-induced bone marrow apoptosis and colony-forming units (CFUs)

(A) The indirect TUNEL method was used to quantify the percent apoptotic cells in lineage negative bone marrow samples derived from CC019 and CC042 mice after sham (blue) or 1-Gy X-ray (green) exposures (n = 6–8 per exposure condition). Bone marrow samples were collected 24 h and 4 weeks after exposure and pooled in sets of two mice.

(B–D) The reconstitution capacity of lineage-negative bone marrow samples derived from CC019 and CC042 mice after sham (blue) or 1-Gy X-ray (green) exposures was quantified. Lineage-negative cells were obtained by removing the following lineage-specific antigens: CD5, CD45R (B220), CD11b, anti-Gr-1 (Ly-6G/C), 7-4, and Ter-119. Total CFUs (B), including granulocyte and macrophage progenitors (G/M/GMs), burst-forming unit erythroid (BFU-E), and granulocyte, erythrocyte, monocyte, megakaryocyte (GEMM); granulocyte and macrophage progenitor CFU (G/M/GM) (C) and erythroid progenitor CFU (burst-forming unit erythroid [BFU-E]) (D) were quantified per 10,000 lineage-negative cells. Error bars indicate standard deviation across biologic replicates. The p values were obtained using Student's t test.

(G/M/GM, BFU-E, and GEMM), and G/M/GM and BFU-E CFUs were quantified based on their morphology. Total and G/M/GM CFUs per 10,000 lineage-negative marrow cells were significantly reduced in CC019 and CC042 strains 24 h after 1 Gy X-ray exposure (Figures 4B and 4C). At 4 weeks after exposure, fewer total CFUs ($p = 0.022$) and G/M/GM CFUs ($p = 0.020$) were observed in the sensitive CC019 strain, whereas in the resistant CC042 strain, no significant difference was observed between irradiated and control mice (Figures 4B and 4C). BFU-E also appeared to be reduced at 24 h after 1 Gy X-ray exposure in both strains, albeit with less statistical significance in CC019 ($p = 0.07$) than in CC042 ($p = 0.02$). Recovery was observed in both strains at 4 weeks after radiation exposure (Figure 4D).

Genetic loci associated with radiation sensitivity

The strain specificity we observed in hematologic phenotypes in the sham cohorts and the ratios of radiation sensitivity suggested that host genetics plays an important role in determining radiation sensitivity. To identify the genetic loci associated with radiation sensitivity, we performed genome-wide association studies (GWASs) using 83,282 single-nucleotide polymorphisms (SNPs) across 33 strains (24-h cohort) or 31 strains (4-week cohort) at 24 h and 4 weeks for 22 hematologic parameters after sham and X-ray radiation exposure. The two sham irradiated cohorts were analyzed separately because the age of the mice was different at the 24-h cohort (12 weeks of age; Table S3) and 4-week cohort (16 weeks of age; Table S5). For the X-ray irradiated cohorts, we used the ratio of all hematologic parameters in irradiated mice over the median values in the sham irradiated mice at 24 h (Table S4) and 4 weeks (Table S6) after exposure.

We then focused our analysis on the GWAS results of the radiation resistance scores we calculated at 24 h (Figure 2C; Table S3) and 4 weeks (Figure 3C; Table S5) after radiation exposure. We identified 145 and 101 SNPs significantly associated with radiation sensitivity at 24 h ($p < 10^{-12}$) and 4 weeks ($p < 10^{-7}$) after radiation exposure, respectively (Figure 5). A lower threshold to identify significant SNPs was employed at 4 weeks after radiation exposure because of a reduced dynamic range across the strains in radiation resistance scores. This analysis revealed a complex association of quantitative trait loci (QTLs) across the genome. At 24 h, we identified 22 QTLs, containing 290 candidate genes, associated with the radiation resistance score ranging in size from 44 kb to 4.4 Mb (Table S7). At 4 weeks, we identified 5 QTLs, containing 99 candidate genes, associated with the radiation resistance score ranging in size from 0.74 to 6.1 Mb (Table 1). To identify candidate genes with potential impact on immune system radiation sensitivity in humans, we compared all genes identified in the mouse radiation resistance score QTLs at 24 h and 4 weeks with human genes identified in GWASs of immune-related diseases or traits. At 24 h, 119 of 290 candidate genes, and at 4 weeks, 47 of 99 candidate genes, were also identified in human GWASs of immune-related diseases or traits (Tables 1 and S7). To further identify potential candidate genes associated with radiation sensitivity, we performed RNA sequencing (RNA-seq) in unirradiated animals comparing the transcriptome in whole blood of radiation-resistant (CC002, CC037, and CC061) and -sensitive (CC015,

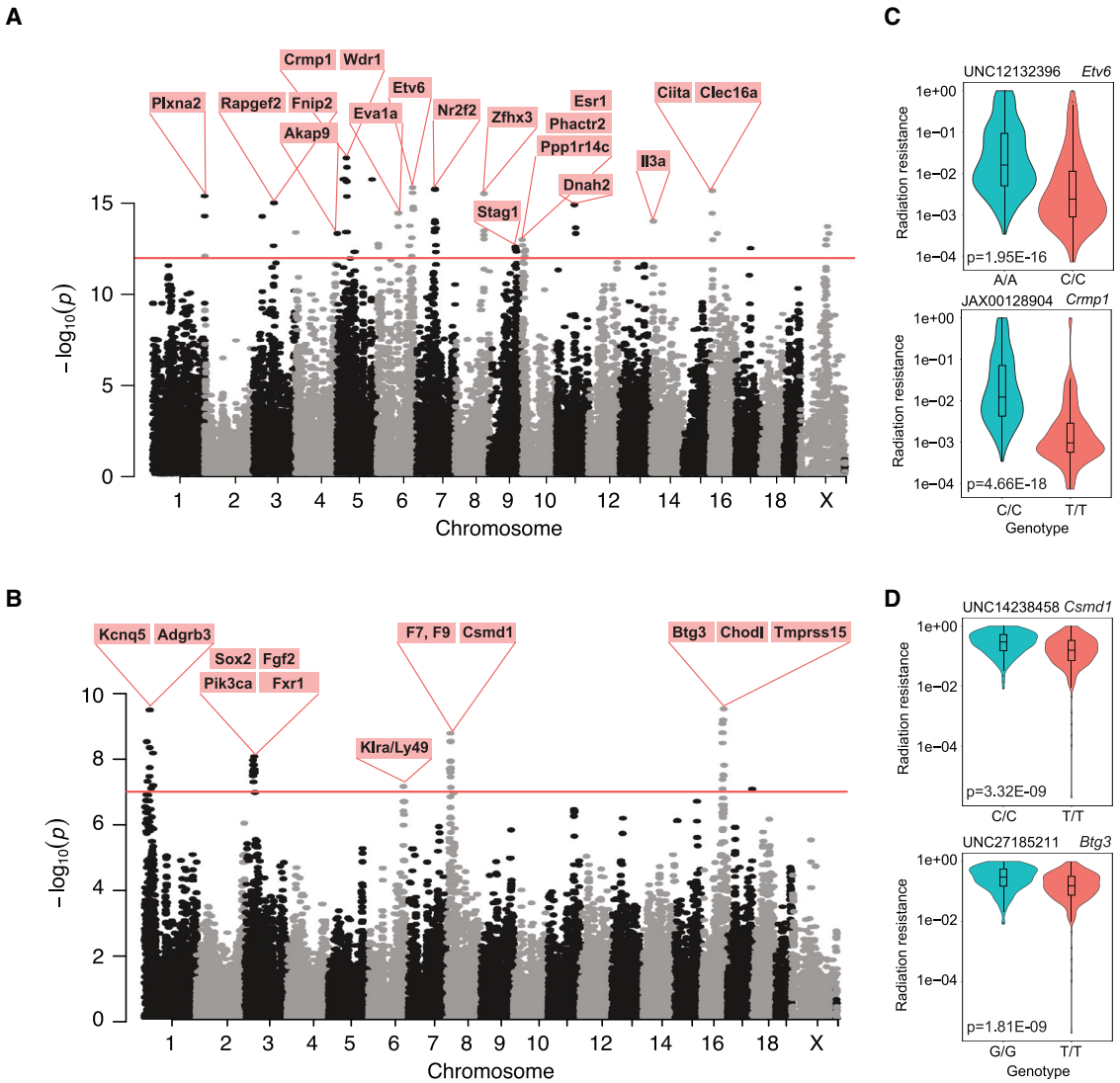

Figure 5. Identification of genetic variations and candidate genes associated with radiation sensitivity in CC mice

(A–D) Manhattan plot of the GWAS analysis for radiation sensitivity in CC mice (n = 351 mice at 24 h and 439 at 4 weeks) at 24 h after radiation exposure (A) and 4 weeks after radiation exposure (B). The $-\log_{10}(p)$ is shown for 83,282 SNPs ordered based on genomic position. The horizontal red line indicates the QTL significance threshold at $-\log_{10}(p) = 12$ (24 h after radiation exposure) and $-\log_{10}(p) = 7$ (4 weeks after radiation exposure). Note the difference in y axis scale between (A) and (C) largely because of immune cell recovery observed at 4 weeks after radiation exposure. Candidate genes previously associated with immune-related processes located in representative QTL are listed above the plot. SNP-specific associations within candidate genes associated with radiation sensitivity at 24 h (C) and 4 weeks (D) after radiation exposure. Box and whisker plots indicate median, 25th and 75th percentiles, 5th and 95th percentiles, and individual samples beyond these limits. Outliers are cases with values beyond 1.5 times the interquartile range. The p values were obtained using the Mann-Whitney test.

CC024, and CC080) strains of mice based on radiation resistance scores calculated at 24 h after radiation exposure (Figure 2C). We identified 766 differentially expressed genes comparing the transcriptome of radiation-sensitive with -resistant strains (adjusted $p < 0.1$; $|\log2 \text{ fold change}| > 0.58$; Table S8). Interestingly, of the 290 candidate genes identified in our radiation resistance QTL analysis at the 24-h time point, we found a significant overlap of 14 genes (representation factor, 3.3; p = 1.3E−04). Of these 14 genes, 4 genes were expressed lower in radiation-resistant strains (*Klrg1*, *Afap1*, *Mrfap1*, and *Dnah2*), whereas the remaining 10 genes (*Gcfc2*, *Wfs1*, *Slc2a3*, *Rmnd1*, *Ercc6l*, *Fam234b*, *Emp1*, *Borcs5*, *Sorcs2*, and *Fam174b*) were expressed higher in radiation-resistant strains compared with radiation-sensitive strains. These data suggest that whole blood transcript levels in unirradiated mice at least partially capture the radiation sensitivity biomarkers identified using our GWAS.

Radiation sensitivity predicts relapse-free survival in medulloblastoma patients

Finally, we investigated whether radiation sensitivity evaluation in mice could predict survival in human cancer patients. We first

Table 1. Genomic locations of QTLs affecting radiation sensitivity 4 weeks after X-ray exposure

QTL	Chromosome	Start (bp)	Starting SNP	Stop (bp)	Ending SNP	Size (Mb)	Candidate genes	Overlap with human GWAS
1	1	20915583	JAX00001337	21657167	UNC252437	0.74	Efhc1, Gsta3, Kcnq5, Khdc1a, Khdc1b, Khdc1c, Paqr8, Tmem14a, Tram2	acute myeloid leukemia: Tmem14a mean platelet volume: PAQR8, EFHC1 neutrophil count/percentage: EFHC1 platelet count: PAQR8, EFHC1, GSTA3 white blood cell count: EFHC1
2	1	33731402	UNC407455	34759027	UNC426583	1.03	Amer3, Arhgef4, Bag2, Bend6, Ccdc115, Cfc1, Dst, Imp4, Prss39, Prss40, Ptpn18, Rab23, Zfp451	mean spheric corpuscular volume: DST red blood cell count: DST
3	3	32307341	UNCHS008338	38413275	UNC5073476	6.11	Acad9, Actl6a, Adad1, Anxa5, Atp11b, Bbs12, Bbs7, Ccdc144b, Ccdc39, Ccna2, Cetn4, Dcun1d1, Dnajc19, Exosc9, Fgf2, Fxr1, Gnb4, Il2, Il21, Kcnmb3, Mccc1, Mfn1, Mrpl47, Ndufb5, Nudt6, Pex5l, Pik3ca, Qrfpr, Sox2, Spata5, Spry1, Trpc3, Ttc14, Usp13, Zfp267, Zfp639, Zmat3	acute myeloid leukemia: USP13, CCDC39, TRPC3 asthma: ADAD1, IL2 celiac: ADAD1, IL2, IL21 Crohn's and IBD: ADAD1, IL2, IL21 eosinophil counts: IL2, IL21 lymphocyte count: MCCC1, BBS12, FGF2, IL21 lymphocyte/monocyte ratio: ACAD9 mean corpuscular hemoglobin: BBS7, PIK3CA, ATP11B, ZMAT3, CCNA2, EXOSC9 mean corpuscular volume: EXOSC9, ZMAT3, PIK3CA, TRPC3 mean platelet volume: ZMAT3, IL2, IL21, QRFPR mean reticulocyte volume: PIK3CA, TRPC3, ZMAT3 mean spheric corpuscular volume: TRPC3, ZMAT3, PIK3CA neutrophil count/percentage: BBS12, FGF2 platelet count: ZMAT3, IL2, IL21 red blood cell count: PIK3CA, EXOSC9, ZMAT3, BBS7 reticulocyte count: ATP11B rheumatoid arthritis; IL2, IL21 type 1 diabetes: IL2, IL21, ADAD1, PEXSL, ANXA5 type 2 diabetes: NUDT6, PEX5L, ANXA5, ACAD9, QRFPR

(*Continued on next page*)

Table 1. *Continued*

QTL	Chromosome	Start (bp)	Starting SNP	Stop (bp)	Ending SNP	Size (Mb)	Candidate genes	Overlap with human GWAS
4	8	12463567	UNCHS022196	16858827	JAX00662205	4.40	Adprhl1, Arhgef10, Atp11a, Atp4b, Cdc16, Cfap97d2, Champ1, Cln8, Coprs, Csmd1, Cul4a, Dcun1d2, Dlgap2, Erich1, F10, F7, Fbxo25, Gas6, Grk1, Grtp1, Kbtbd11, Lamp1, Mcf2l, Myom2, Pcid2, Proz, Rasa3, Spaca7, Tdrp, Tfdp1, Tmco3, Tmem255b, Tubgcp3, Upf3a	acute myeloid leukemia: CLN8, CSMD1, DLGAP2 hematocrit: GAS6 hemoglobin: GAS6 lymphocyte count: CFAP97D2, RASA3, GAS6 lymphocyte/monocyte ratio: RASA3 neutrophil count/percentage: TMCO3, CUL4A, DCUN1D2, CFAP97D2 monocyte count/percentage: RASA3, CFAP97D2, DCUN1D2, CDC16 mean corpuscular hemoglobin: ATP11A, CUL4A, TMCO3, PCID2 mean reticulocyte volume: CSMD1, CUL4A, TMCO3, GAS6 mean spheric corpuscular volume: ATP11A, CUL4A, TFDP1, GAS6 red blood cell count: ATP11A, GAS6, TFDP1 reticulocyte count: F10 mean corpuscular volume: ATP11A, PCID2, CUL4A, TFPD1 mean platelet volume: MCF2L, CUL4A, GRTP1 platelet count: GRTP1, ADPRHL1, ATP11A type 2 diabetes: CSMD1, MYOM2 white blood cell count: TMCO3, RASA3, CFAP97D2, CUL4A
5	16	78080715	UNCHS043153	84200913	UNC27278078	6.12	Btg3, Chodl, Cxadr, Ncam2, Tmprss15	asthma: TMPRSS15, NCAM2 mean corpuscular volume: CXADR neutrophil count/percentage: CXADR white blood cell count: CXADR

Candidate genes within QTL are listed. Overlapping genes with human genome-wide association studies of immunologic traits are indicated.
FGF, fibroblast growth factor; IBD, inflammatory bowel disease; IL, interleukin.

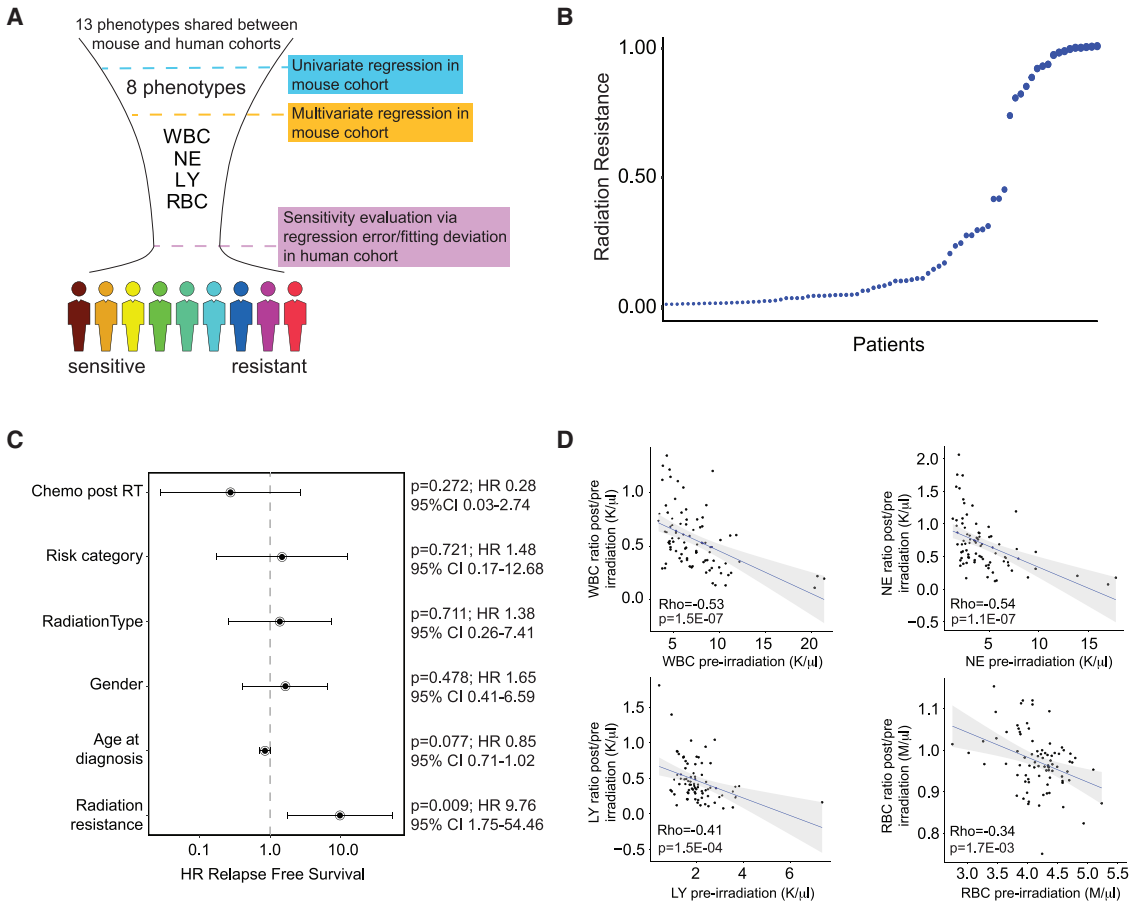

Figure 6. Mouse-derived radiation sensitivity score predicts relapse-free survival in medulloblastoma patients

(A) Hematologic parameters associated with radiation exposure were determined by univariate and multivariate analyses in the mouse cohort using 13 hematologic parameters in common between the mouse and human cohorts. Hematologic radiation sensitivity and resistance were then determined by sensitivity evaluation via regression error/fitting deviation in the human medulloblastoma patient cohort.

(B) Radiation resistance score for all medulloblastoma patients (n = 80) based on four hematologic parameters.

(C) Multivariate Cox regression analysis of independent prognostic factors. Values indicate the hazard ratio for relapse-free survival. Error bars indicate 95% confidence intervals (CIs). The p values were obtained using multivariate CoxPH regression.

(D) Spearman's rank correlation and p value of four hematologic parameters in medulloblastoma patients comparing pre-irradiation values and the ratio of values after the first week of radiotherapy over pre-irradiation values.

filtered the complete blood count data in the cohort of 99 patients diagnosed with medulloblastoma to include those that were shared between the mouse and human cohorts.[9] The MPV and RDW parameters were removed for downstream analysis because of incomplete data in the human cohort. The remaining 13 immune parameters were shared between the mouse and human cohorts. A combined univariate and multivariate analysis identified WBC, neutrophil, lymphocyte, and red blood cell counts to be significantly associated with radiation exposure in the mouse cohort (Figure 6A). We then calculated for each patient the ratio for each immune parameter before and after the first week of radiotherapy treatment (n = 80 patients remained because of missing values). Using the four immune parameters identified in our mouse cohort, we then performed radiation sensitivity evaluation and assigned a radiation resistance score to each patient via regression error fitting deviation analysis using 10,000 bootstrapping iterations and a sampling rate of 60% (Figure 6B). Similar to our mouse cohort results, we observed a wide range in radiation resistance across patients. Interestingly, radiation resistance was unfavorably and significantly associated with relapse-free survival (p = 0.009; hazard ratio = 9.76; 95% confidence interval [CI]: 1.75–54.46; Figure 6C) independent of other clinical factors, including age at diagnosis, gender, radiation type (proton or photon irradiation), risk category (high risk vs. standard risk), and the use of chemotherapy post-radiotherapy. These data suggest that patients with a high hematologic radiation resistance score are at increased risk of relapse after radiotherapy treatment. Because our resistance score is based on ratios, we investigated the correlation between the ratios of the four immune parameters across the human cohort and individual patient pre-irradiation levels. We observed significant negative correlations between the pre-irradiation levels of all four phenotypes (WBC, neutrophil, lymphocyte, and red blood cell counts) and the ratio calculated

1 week after the first week of radiotherapy (Figure 6D; correlation coefficient < −0.34; p < 1.7E−03 by non-parametric Spearman's rank test). Negative correlations were also observed in our 24-h mouse cohort between sham levels of WBC, neutrophil, and lymphocyte counts and the ratios calculated 24 h after radiation exposure (Figure S4). Taken together, these data suggest that high pre-irradiation immune counts indicate increased radiosensitivity and reduced risk of relapse.

DISCUSSION

Depletion of circulating blood cells, hematologic toxicity, is a common adverse event during and after multimodal cancer therapy. Lymphocytes are the most radiosensitive cells of the hematopoietic system. Hematologic toxicity, and in particular radiation-induced depletion of circulating lymphocyte counts, has a significant negative impact on overall survival outcomes for many solid cancers.[2–6] This suggests that the immune system plays an important role in improving the efficacy of radiation therapy. Our study investigated the effect of genetic background on radiotherapy-induced hematologic toxicity with the goal of identifying novel targets to predict, and ultimately prevent and ameliorate, this harm in order to improve patient outcome.

The human immune system functions to fight disease and consists of a complex network of cells, tissues, and organs, which closely work together in maintaining optimal health. Abundance levels of lymphocyte populations are tightly regulated to maintain immune cell homeostasis by balancing cell proliferation and programmed cell death. Genetic variants are well known to influence the immune system and immune responses, which in turn can influence susceptibility to immune system disorders, including allergies, asthma, immune-deficiency diseases, and autoimmune diseases.[10] Moreover, many disorders that were initially not believed to be linked to the immune system (e.g., obesity and insulin resistance) are now causally linked to inflammatory processes and immune cell mobilization. Understanding the genes affecting immune system cells and treatment-associated hematologic toxicity is the first step in developing novel therapies that are personalized according to an individual's genetic make-up. We provide a resource for identifying genes that critically modulate the impact of radiation on blood cell counts.

A number of studies have investigated the association of genetic variants and radiotherapy toxicity. However, most studies involved small patient numbers and lacked replication (reviewed in West and Barnett[11]). Also, most human studies are retrospective in nature, and the contribution of other factors, such as chemotherapy, to alterations in lymphocyte counts is difficult to clarify. The study of high-penetrance genes, which confer genetic predisposition to immune system disorders in certain rare human families, has been very successful, but it is likely that low-penetrance genes present at high frequency in the human population are major genetic components that contribute to radiation-induced hematologic toxicity.[12,13]

We carried out a study to identify loci that correlate with blood counts after radiotherapy in a large multi-parental panel of recombinant inbred strains, the "Collaborative Cross" (CC), a population of mice that contains a level of genetic and phenotypic diversity on par with the human population.[14–16] We and others have used the CC to identify genetic factors contributing to a wide variety of phenotypic endpoints, including cancer risk, memory, anxiety, gut microbiome composition, biologic responses to carcinogens and tobacco, and viral infection.[17–23] Several studies have probed the immune system in incipient lines of the CC (pre-CC), CC lines, and F1 crosses of CC strains and reported strong contributions of host genetics on the immune system,[24–27] confirming that the CC is a useful resource for identifying immunologic traits. To identify QTLs associated with immune sensitivity, our study focused on basic immunophenotyping using a quantitative hematology analyzer supplemented with lymphocyte subset analysis for B cell (CD45R/B220) and T cell (CD3/CD4/CD8) counts across 35 CC strains exposed to 1 Gy of X-rays and compared with sham-exposed matched animals.

By combining our QTL analyses with RNA-seq analysis, we identified 14 genes that were associated with the acute effects of ionizing radiation on blood cells: prior work had implicated seven of these genes as potential mediators of radiation response, whereas, to our knowledge, the remaining seven of these genes, *Afap1*, *Ercc6l*, *Slc2a3*, *Rmnd1*, *Fam234b*, *Fam174b*, and *Emp1*, are novel mediators of radiosensitivity.

The seven previously implicated genes are *Klrg1*, *Mrfap1*, *Dnah2*, *Gcfc2*, *Wfs1*, *Borcs5*, and *Sorcs2*; prior work has suggested roles for each in radiation response, radiation resistance, and/or DNA repair. *Klrg1* is an immune checkpoint receptor inhibiting T and natural killer (NK) cell activity,[28] and its expression increased on T cells after radiotherapy in patients with locally advanced nasopharyngeal carcinoma.[29] Our QTL analysis of ratios of immune phenotypes from irradiated over sham irradiated animals confirmed that the *Klrg1* locus is significantly associated with lymphocyte, B cell, and T cell subpopulations. *MRFAP1* was identified in a genome-wide RNAi screen as being required for resistance to ionizing radiation.[30] *DNAH2* plays a potential role in the homologous recombination DNA-repair pathway,[31] and mutations have been observed in several Fanconi anemia patients, who are sensitive to DNA-damaging agents, including radiation.[32] Of additional interest, *DNAH2* was found to be mutated in >10% of chronic myelomonocytic leukemia patients,[33] and knockout mice showed abnormal lymph node morphology.[34] *GCFC2* was identified in a single-cell transcriptome study identifying radioresistance genes in esophageal squamous cell carcinoma and was further identified as a transcription factor contributing to radiation resistance in hepatocellular carcinoma.[35,36] *Wfs1* is primarily expressed in the endoplasmic reticulum and was shown to be downregulated in the hippocampus of mice after exposure to ionizing radiation.[37] *BORCS5* has been shown to play a role in cancer cell radiation resistance and invasion mediated by Sp1, a transcription factor that is activated in an ATM-dependent manner after radiation exposure.[38] *Sorcs2* loss has been associated with elevated levels of double-stranded DNA breaks in the mouse dentate gyrus[39] and has been shown to be upregulated after radiation exposure of human pulmonary alveolar epithelial cells.[40]

Using our regression analysis pipeline to determine radiation sensitivity in a human medulloblastoma cohort, we identified four parameters in our mouse cohort associated with radiation

sensitivity (WBC, neutrophil count, lymphocyte count, and red blood cell count). Using these mouse-derived parameters, we were then able to calculate radiation resistance scores in the human patient cohort based on blood counts collected after the first week of radiotherapy. Interestingly, we found that radiation resistance, defined as the least change in blood counts 1 week after the first week of treatment compared with pre-irradiation levels, was associated with higher risk of relapse. Further analyses showed that pre-irradiation levels for these four parameters were negatively correlated with the percentage-level reduction in blood counts, and that patients with the highest baseline levels (who exhibited the largest percent reduction in counts) were less likely to have a relapse of their medulloblastoma (that is, compared with patients with the lowest baseline levels, who percentage-wise showed a lesser reduction in blood counts after radiotherapy). Interestingly, for three of the four parameters (WBC, neutrophil, and red blood cell counts), the same negative correlation was observed across the CC. Taken together, our analysis identified high blood counts of four parameters as a potential biomarker for predicting disease relapse in a multi-institutional cohort of medulloblastoma patients treated with radiation therapy. Interestingly, 1 of the 14 genes identified in our combined QTL and RNA-seq analysis, *Fam234b*, controls blood immune cell levels because a comparison of blood counts in *Fam234b* knockout mice with wild-type controls showed decreased T cells and $CD8^+$ T cells in female mice and increased B cells in male mice.[34]

Our analyses identified sex differences comparing baseline immune parameters and radiation responses between male and female mice, suggesting that assessment of radiation sensitivity should take sex into consideration. There are notable sex differences in immune cell phenotypes and inflammatory responses. For example, overall hospital mortality was significantly lower in women in a matched cohort study of men with severe sepsis,[41] and women have a higher incidence of auto-immune conditions compared with men.[42] Although the heightened inflammatory response is advantageous in response to infection and sepsis, it can be detrimental in immune responses against self, resulting in an increased rate of auto-immune disorders in women. We also observed sex differences at the population level. We observed that peripheral blood in male mice contains fewer circulating T cells compared with female mice. After radiation exposure, this difference was maintained. We also observed sex differences in PLT counts and MPV. PLT levels were higher in male mice compared with female mice, whereas the MPV was higher in female mice compared with male mice. In contrast, in the human population, PLT counts are higher in females than in males.[43,44] PLT counts and MPV levels remained unaffected 24 h after radiation exposure in both male and female mice compared with sham irradiated mice. However, at 4 weeks after radiation exposure, PLT counts were significantly reduced in both male and female mice compared with age-matched controls. This observation is consistent with prior observations and likely due to delayed radiation effects on non-nucleated blood components.[45] Finally, we observed a significant sex difference in the recovery of myeloid counts 4 weeks after radiation exposure. Although levels in irradiated male mice were not different from sham irradiated mice, levels in irradiated female mice remained significantly lower compared with sham irradiated mice. In our sex-dependent radiation sensitivity analysis at 4 weeks after exposure, myeloid cell counts were included in the radiation sensitivity panel in female mice, but not male mice. Moreover, the sex-combined radiation sensitivity CC strain ranking was significantly correlated with female radiation sensitivity, but not male radiation sensitivity. These data suggest that women may be more vulnerable to prolonged neutropenia following radiotherapy; this possibility is consistent with a report that showed that severe side effects from cancer treatments, including chemotherapy, targeted therapy, and immunotherapy, are more common in women than in men.[46]

Our genetic association analyses focused on the radiation-resistant scores calculated using a combination of a univariate and multi-variate approach followed by error-fitting deviation analysis. Genetic analyses of all 22 immunophenotypes individually in sham irradiated mice at 12 and 16 weeks of age and the ratios comparing irradiated with sham irradiated mice identified many QTLs associated with baseline immune parameter levels and radiation sensitivity (Tables S3, S4, S5, and S6). For example, QTL analysis of the ratio of $CD4^+$ T cell counts over levels in sham irradiated mice at 24 h after exposure revealed strong genetic linkage on chromosomes 5 and 6. The QTLs on mouse chromosome (m) 5 include *Hgf*, *Gnai1*, *Sema3c*, and *CD36*, whereas the QTL on m6 was also identified using the radiation resistance score as a trait for linkage analysis. The QTL m5 showed strong linkage for T, $CD4^+$, and $CD8^+$ T cells, with weaker linkage for B cells. A human GWAS has reported linkage between *CD36* (on human chromosome [h] 7) and leukocyte counts.[47] The QTL on m6 also showed strong linkage for T cell, $CD8^+$ T cell, B cell, and lymphocyte counts. The QTL was slightly larger than identified using the radiation resistance score and includes *Glcci1*, which has been shown to play an important role in apoptosis regulation of thymic T cells.[48] Our data show that *Glcci1* could more generally play an important role in radiation-induced apoptosis in T cells and B cells. In human GWASs, GLCCI1 has been associated with leukocyte and granulocyte counts and acute myeloid leukemia.[49–51]

Limitations of the study

It will be useful to expand the immunophenotyping marker set in a subset of resistant and sensitive CC strains to further probe radiation sensitivity by including markers to delineate B cell progenitors, as well as transitional, marginal zone, and follicular B cells (CD19, CD21, CD23, CD25, CD43, IgM, IgD), naive, effector and memory T cells (CD44, CD62L), and T regulatory cells (CD25, FOXP3). Our study focused on a single, whole-body X-ray exposure. Fractionated radiation regimen and partial body exposures could be tested to mimic other human radiotherapy conditions more closely. Also, other radiation environments, including protons, high-linear energy transfer (LET) ionizing radiation from heavy ions, and mixed exposures, could be considered. Our study irradiated all animals at 12 weeks of age, the life phase equivalent for a 20-year-old human. Age-related changes in oxidative stress, telomere length, inflammatory responses, and cell functions can alter the radiation risk profile for individual strains of mice and potentially the QTLs associated with radiation sensitivity.[52,53] Future studies

across the life span will need to be conducted to address whether the radiation resistance score is influenced by age at exposure. Lastly, our analysis did not incorporate the potential role of the gut microbiome in baseline immune level variations or radiation sensitivity phenotypes. Even though, in this study, all mice were bred and maintained in the same built environment, host genetics is known to influence the composition of the murine gut microbiome. Future studies will investigate the interaction of host genetics and the gut microbiome in mediating the radiation response. Nonetheless, our study provides basic immunophenotyping across the CC at two time points after X-ray exposure and will be a valuable resource for investigating risk associated with radiation exposure in a wide variety of settings, including medical exposures associated with diagnostic and therapeutic procedures, occupational exposures to nuclear plant workers, waste managers and medical workers, exposures associated with space exploration, nuclear power plant incidents, and exposures associated with the risk of a terrorist attack with radiologic or nuclear devices. Given the prior observation that 7 of the 14 genes we identified herein have been previously linked to radiation response, it appears likely that the 7 novel genes we identified also play important roles in post-radiation processes. Moreover, on the basis of this prior work and on our findings, we hypothesize that measuring gene expression levels of these 14 genes prior to radiotherapy will enable identification of patients at highest risk for hematologic toxicity.

STAR★METHODS

Detailed methods are provided in the online version of this paper and include the following:

- KEY RESOURCES TABLE
- RESOURCE AVAILABILITY
  - Lead contact
  - Materials availability
  - Data and code availability
- EXPERIMENTAL MODEL AND SUBJECT DETAILS
  - CC mice experiments
- METHOD DETAILS
  - Mice and radiation exposure
  - Mouse blood analysis
  - Isolation of mouse hematopoietic stem cells and granulocyte macrophage-colony forming unit (GM-CFU) assay
  - Apoptosis assay
  - Radiation resistance score
  - Genome-wide association analysis
  - RNA isolation and sequencing
  - Radiation resistance score transfer from mouse to human
  - Medulloblastoma patient cohort
- QUANTIFICATION AND STATISTICAL ANALYSIS

SUPPLEMENTAL INFORMATION

Supplemental information can be found online at https://doi.org/10.1016/j.xgen.2023.100422.

ACKNOWLEDGMENTS

The authors would like to thank Dr. Sasha A. Langley for initial analyses of the mouse cohort. This work was supported by NIAID 1R21AI145390 (to A.M.S.). Additional support was provided by the Department of Defense (DoD) BCRP (BC190820 to J.-H.M.) and the DOE Low Dose Radiation SFA (A.M.S. and J.-H.M.). Lawrence Berkeley National Laboratory (LBNL) is a multi-program laboratory operated by the University of California for the DOE under contract DE AC02-05CH11231. We thank staff at the LBNL Animal Facility for maintenance of CC mice. We thank the UCLA Technology Center for Genomics & Bioinformatics for RNA-seq services.

AUTHOR CONTRIBUTIONS

J.-H.M., A.M.S., and S.C.K. conceptualized and designed the study. L.H., C.Z., J.L.I., A.M.S., and J.-H.M. performed the animal experiments. H.C. performed formal analysis, including bioinformatics and statistical analyses. M.I.-I., K.X.L., D.H.-K., and S.M.M. collected clinical data. A.M.S., J.-H.M., H.C., J.L.I., S.E.C., D.W.T., M.I.-I., K.X.L., D.H.-K., S.M.M., and S.C.K. were involved in critical review of the data and interpretation of results. A.M.S., J.-H.M., H.C., J.L.I., and S.C.K. created the manuscript figures and supplemental information. A.M.S. drafted the manuscript. All authors edited, reviewed, revised, and approved the manuscript text. J.-H.M. and A.M.S. acquired funding for the study.

DECLARATION OF INTERESTS

The authors declare no competing interests.

INCLUSION AND DIVERSITY

We support inclusive, diverse, and equitable conduct of research.

Received: May 8, 2023
Revised: August 19, 2023
Accepted: September 12, 2023
Published: October 6, 2023

REFERENCES

1. Baskar, R., Lee, K.A., Yeo, R., and Yeoh, K.W. (2012). Cancer and radiation therapy: current advances and future directions. Int. J. Med. Sci. *9*, 193–199. https://doi.org/10.7150/ijms.3635.
2. Grossman, S.A., Ye, X., Lesser, G., Sloan, A., Carraway, H., Desideri, S., and Piantadosi, S.; NABTT CNS Consortium (2011). Immunosuppression in patients with high-grade gliomas treated with radiation and temozolomide. Clin. Cancer Res. *17*, 5473–5480. https://doi.org/10.1158/1078-0432.CCR-11-0774.
3. Balmanoukian, A., Ye, X., Herman, J., Laheru, D., and Grossman, S.A. (2012). The association between treatment-related lymphopenia and survival in newly diagnosed patients with resected adenocarcinoma of the pancreas. Cancer Invest. *30*, 571–576. https://doi.org/10.3109/07357907.2012.700987.
4. Campian, J.L., Ye, X., Brock, M., and Grossman, S.A. (2013). Treatment-related lymphopenia in patients with stage III non-small-cell lung cancer. Cancer Invest. *31*, 183–188. https://doi.org/10.3109/07357907.2013.767342.
5. Grossman, S.A., Ellsworth, S., Campian, J., Wild, A.T., Herman, J.M., Laheru, D., Brock, M., Balmanoukian, A., and Ye, X. (2015). Survival in Patients With Severe Lymphopenia Following Treatment With Radiation and Chemotherapy for Newly Diagnosed Solid Tumors. J. Natl. Compr. Cancer Netw. *13*, 1225–1231.
6. Wild, A.T., Ye, X., Ellsworth, S.G., Smith, J.A., Narang, A.K., Garg, T., Campian, J., Laheru, D.A., Zheng, L., Wolfgang, C.L., et al. (2015). The Association Between Chemoradiation-related Lymphopenia and Clinical Outcomes in Patients With Locally Advanced Pancreatic Adenocarcinoma.

Am. J. Clin. Oncol. *38*, 259–265. https://doi.org/10.1097/COC.0b013e3182940ff9.

7. Collaborative Cross Consortium (2012). The genome architecture of the Collaborative Cross mouse genetic reference population. Genetics *190*, 389–401. https://doi.org/10.1534/genetics.111.132639.
8. Wilkins, R.C., Kutzner, B.C., Truong, M., and McLean, J.R.N. (2002). The effect of the ratio of CD4+ to CD8+ T-cells on radiation-induced apoptosis in human lymphocyte subpopulations. Int. J. Radiat. Biol. *78*, 681–688. https://doi.org/10.1080/09553000210144475.
9. Liu, K.X., Ioakeim-Ioannidou, M., Susko, M.S., Rao, A.D., Yeap, B.Y., Snijders, A.M., Ladra, M.M., Vogel, J., Zaslowe-Dude, C., Marcus, K.J., et al. (2021). A Multi-institutional Comparative Analysis of Proton and Photon Therapy-Induced Hematologic Toxicity in Patients With Medulloblastoma. Int. J. Radiat. Oncol. Biol. Phys. *109*, 726–735. https://doi.org/10.1016/j.ijrobp.2020.09.049.
10. Roederer, M., Quaye, L., Mangino, M., Beddall, M.H., Mahnke, Y., Chattopadhyay, P., Tosi, I., Napolitano, L., Terranova Barberio, M., Menni, C., et al. (2015). The genetic architecture of the human immune system: a bioresource for autoimmunity and disease pathogenesis. Cell *161*, 387–403. https://doi.org/10.1016/j.cell.2015.02.046.
11. West, C.M., and Barnett, G.C. (2011). Genetics and genomics of radiotherapy toxicity: towards prediction. Genome Med. *3*, 52. https://doi.org/10.1186/gm268.
12. Shields, P.G., and Harris, C.C. (2000). Cancer risk and low-penetrance susceptibility genes in gene-environment interactions. J. Clin. Oncol. *18*, 2309–2315.
13. Ewart-Toland, A., and Balmain, A. (2004). The genetics of cancer susceptibility: from mouse to man. Toxicol. Pathol. *32* (*Suppl 1*), 26–30.
14. Zou, F., Gelfond, J.A.L., Airey, D.C., Lu, L., Manly, K.F., Williams, R.W., and Threadgill, D.W. (2005). Quantitative trait locus analysis using recombinant inbred intercrosses: theoretical and empirical considerations. Genetics *170*, 1299–1311. https://doi.org/10.1534/genetics.104.035709.
15. Threadgill, D.W., Hunter, K.W., and Williams, R.W. (2002). Genetic dissection of complex and quantitative traits: from fantasy to reality via a community effort. Mamm. Genome *13*, 175–178. https://doi.org/10.1007/s00335-001-4001-Y.
16. Churchill, G.A., Airey, D.C., Allayee, H., Angel, J.M., Attie, A.D., Beatty, J., Beavis, W.D., Belknap, J.K., Bennett, B., Berrettini, W., et al. (2004). The Collaborative Cross, a community resource for the genetic analysis of complex traits. Nat. Genet. *36*, 1133–1137. https://doi.org/10.1038/ng1104-1133.
17. He, L., Wang, P., Schick, S.F., Huang, A., Jacob, P., 3rd, Yang, X., Xia, Y., Snijders, A.M., Mao, J.H., Chang, H., and Hang, B. (2021). Genetic background influences the effect of thirdhand smoke exposure on anxiety and memory in Collaborative Cross mice. Sci. Rep. *11*, 13285. https://doi.org/10.1038/s41598-021-92702-1.
18. Jin, X., Zhang, Y., Celniker, S.E., Xia, Y., Mao, J.H., Snijders, A.M., and Chang, H. (2021). Gut microbiome partially mediates and coordinates the effects of genetics on anxiety-like behavior in Collaborative Cross mice. Sci. Rep. *11*, 270. https://doi.org/10.1038/s41598-020-79538-x.
19. Mao, J.H., Kim, Y.M., Zhou, Y.X., Hu, D., Zhong, C., Chang, H., Brislawn, C.J., Fansler, S., Langley, S., Wang, Y., et al. (2020). Genetic and metabolic links between the murine microbiome and memory. Microbiome *8*, 53. https://doi.org/10.1186/s40168-020-00817-w.
20. Snijders, A.M., Langley, S.A., Kim, Y.M., Brislawn, C.J., Noecker, C., Zink, E.M., Fansler, S.J., Casey, C.P., Miller, D.R., Huang, Y., et al. (2016). Influence of early life exposure, host genetics and diet on the mouse gut microbiome and metabolome. Nat. Microbiol. *2*, 16221. https://doi.org/10.1038/nmicrobiol.2016.221.
21. Wang, P., Wang, Y., Langley, S.A., Zhou, Y.X., Jen, K.Y., Sun, Q., Brislawn, C., Rojas, C.M., Wahl, K.L., Wang, T., et al. (2019). Diverse tumour susceptibility in Collaborative Cross mice: identification of a new mouse model for human gastric tumourigenesis. Gut *68*, 1942–1952. https://doi.org/10.1136/gutjnl-2018-316691.
22. Zhong, C., He, L., Lee, S.Y., Chang, H., Zhang, Y., Threadgill, D.W., Yuan, Y., Zhou, F., Celniker, S.E., Xia, Y., et al. (2021). Host genetics and gut microbiota cooperatively contribute to azoxymethane-induced acute toxicity in Collaborative Cross mice. Arch. Toxicol. *95*, 949–958. https://doi.org/10.1007/s00204-021-02972-x.
23. Noll, K.E., Whitmore, A.C., West, A., McCarthy, M.K., Morrison, C.R., Plante, K.S., Hampton, B.K., Kollmus, H., Pilzner, C., Leist, S.R., et al. (2020). Complex Genetic Architecture Underlies Regulation of Influenza-A-Virus-Specific Antibody Responses in the Collaborative Cross. Cell Rep. *31*, 107587. https://doi.org/10.1016/j.celrep.2020.107587.
24. Collin, R., Balmer, L., Morahan, G., and Lesage, S. (2019). Common Heritable Immunological Variations Revealed in Genetically Diverse Inbred Mouse Strains of the Collaborative Cross. J. Immunol. *202*, 777–786. https://doi.org/10.4049/jimmunol.1801247.
25. Philip, V.M., Sokoloff, G., Ackert-Bicknell, C.L., Striz, M., Branstetter, L., Beckmann, M.A., Spence, J.S., Jackson, B.L., Galloway, L.D., Barker, P., et al. (2011). Genetic analysis in the Collaborative Cross breeding population. Genome Res. *21*, 1223–1238. https://doi.org/10.1101/gr.113886.110.
26. Phillippi, J., Xie, Y., Miller, D.R., Bell, T.A., Zhang, Z., Lenarcic, A.B., Aylor, D.L., Krovi, S.H., Threadgill, D.W., de Villena, F.P.M., et al. (2014). Using the emerging Collaborative Cross to probe the immune system. Gene Immun. *15*, 38–46. https://doi.org/10.1038/gene.2013.59.
27. Graham, J.B., Swarts, J.L., Mooney, M., Choonoo, G., Jeng, S., Miller, D.R., Ferris, M.T., McWeeney, S., and Lund, J.M. (2017). Extensive Homeostatic T Cell Phenotypic Variation within the Collaborative Cross. Cell Rep. *21*, 2313–2325. https://doi.org/10.1016/j.celrep.2017.10.093.
28. Greenberg, S.A., Kong, S.W., Thompson, E., and Gulla, S.V. (2019). Co-inhibitory T cell receptor KLRG1: human cancer expression and efficacy of neutralization in murine cancer models. Oncotarget *10*, 1399–1406. https://doi.org/10.18632/oncotarget.26659.
29. Qian, H., Dong, D., Fan, P., Feng, Y., Peng, Y., Yao, X., and Wang, R. (2022). Expression of KLRG1 on subpopulations of lymphocytes in the peripheral blood of patients with locally advanced nasopharyngeal carcinoma and prognostic analysis. Precision Radiation Oncology *6*, 199–208. https://doi.org/10.1002/pro6.1165.
30. Hurov, K.E., Cotta-Ramusino, C., and Elledge, S.J. (2010). A genetic screen identifies the Triple T complex required for DNA damage signaling and ATM and ATR stability. Genes Dev. *24*, 1939–1950. https://doi.org/10.1101/gad.1934210.
31. Chang, L., Gao, X., Wang, Y., Huang, C., Gao, M., Wang, X., Liu, C., Wu, W., An, W., Wan, Y., et al. (2021). DNAH2 facilitates the homologous recombination repair of Fanconi anemia pathway through modulating FANCD2 ubiquitination. Blood Sci. *3*, 71–77. https://doi.org/10.1097/BS9.0000000000000076.
32. Chang, L., Yuan, W., Zeng, H., Zhou, Q., Wei, W., Zhou, J., Li, M., Wang, X., Xu, M., Yang, F., et al. (2014). Whole exome sequencing reveals concomitant mutations of multiple FA genes in individual Fanconi anemia patients. BMC Med. Genom. *7*, 24. https://doi.org/10.1186/1755-8794-7-24.
33. Mason, C.C., Khorashad, J.S., Tantravahi, S.K., Kelley, T.W., Zabriskie, M.S., Yan, D., Pomicter, A.D., Reynolds, K.R., Eiring, A.M., Kronenberg, Z., et al. (2016). Age-related mutations and chronic myelomonocytic leukemia. Leukemia *30*, 906–913. https://doi.org/10.1038/leu.2015.337.
34. Groza, T., Gomez, F.L., Mashhadi, H.H., Muñoz-Fuentes, V., Gunes, O., Wilson, R., Cacheiro, P., Frost, A., Keskivali-Bond, P., Vardal, B., et al. (2023). The International Mouse Phenotyping Consortium: comprehensive knockout phenotyping underpinning the study of human disease. Nucleic Acids Res. *51*, D1038–D1045. https://doi.org/10.1093/nar/gkac972.
35. Wu, H., Yu, J., Kong, D., Xu, Y., Zhang, Z., Shui, J., Li, Z., Luo, H., and Wang, K. (2019). Population and single-cell transcriptome analyses reveal diverse transcriptional changes associated with radioresistance in

esophageal squamous cell carcinoma. Int. J. Oncol. *55*, 1237–1248. https://doi.org/10.3892/ijo.2019.4897.

36. Yang, C., Yin, L., Zhou, P., Liu, X., Yang, M., Yang, F., Jiang, H., and Ding, K. (2016). Transcriptional regulation of IER5 in response to radiation in HepG2. Cancer Gene Ther. *23*, 61–65. https://doi.org/10.1038/cgt.2016.1.
37. Langhnoja, J., and Mustak, M. (2019). Gamma-Radiation-Induced Endoplasmic Reticulum Stress and Downregulation of WFS1, Nectin 3, and Sostdc1 Gene Expression in Mice Hippocampus. Basic Clin. Neurosci. *10*, 383–392. https://doi.org/10.32598/bcn.9.10.205.
38. Wu, P.H., Onodera, Y., Giaccia, A.J., Le, Q.T., Shimizu, S., Shirato, H., and Nam, J.M. (2020). Lysosomal trafficking mediated by Arl8b and BORC promotes invasion of cancer cells that survive radiation. Commun. Biol. *3*, 620. https://doi.org/10.1038/s42003-020-01339-9.
39. Gospodinova, K.O., Olsen, D., Kaas, M., Anderson, S.M., Phillips, J., Walker, R.M., Bermingham, M.L., Payne, A.L., Giannopoulos, P., Pandya, D., et al. (2023). Loss of SORCS2 is Associated with Neuronal DNA Double-Strand Breaks. Cell. Mol. Neurobiol. *43*, 237–249. https://doi.org/10.1007/s10571-021-01163-7.
40. Zhong, Y., Lin, Z., Lu, J., Lin, X., Xu, W., Wang, N., Huang, S., Wang, Y., Zhu, Y., Chen, Z., and Lin, S. (2019). CCL2-CCL5/CCR4 contributed to radiation-induced epithelial-mesenchymal transition of HPAEpiC cells via the ERK signaling pathways. Am. J. Transl. Res. *11*, 733–743.
41. Adrie, C., Azoulay, E., Francais, A., Clec'h, C., Darques, L., Schwebel, C., Nakache, D., Jamali, S., Goldgran-Toledano, D., Garrouste-Orgeas, M., et al. (2007). Influence of gender on the outcome of severe sepsis: a reappraisal. Chest *132*, 1786–1793. https://doi.org/10.1378/chest.07-0420.
42. Kronzer, V.L., Bridges, S.L., Jr., and Davis, J.M., 3rd. (2021). Why women have more autoimmune diseases than men: An evolutionary perspective. Evol. Appl. *14*, 629–633. https://doi.org/10.1111/eva.13167.
43. Segal, J.B., and Moliterno, A.R. (2006). Platelet counts differ by sex, ethnicity, and age in the United States. Ann. Epidemiol. *16*, 123–130. https://doi.org/10.1016/j.annepidem.2005.06.052.
44. Stevens, R.F., and Alexander, M.K. (1977). A sex difference in the platelet count. Br. J. Haematol. *37*, 295–300. https://doi.org/10.1111/j.1365-2141.1977.tb06847.x.
45. DiCarlo, A.L., Poncz, M., Cassatt, D.R., Shah, J.R., Czarniecki, C.W., and Maidment, B.W. (2011). Medical countermeasures for platelet regeneration after radiation exposure. Report of a Workshop and Guided Discussion Sponsored by the, *176* (National Institute of Allergy and Infectious Diseases), pp. e0001–e0015, March 22-23, 2010. https://doi.org/10.1667/rrol01.1.
46. Unger, J.M., Vaidya, R., Albain, K.S., LeBlanc, M., Minasian, L.M., Gotay, C.C., Henry, N.L., Fisch, M.J., Lee, S.M., Blanke, C.D., and Hershman, D.L. (2022). Sex Differences in Risk of Severe Adverse Events in Patients Receiving Immunotherapy, Targeted Therapy, or Chemotherapy in Cancer Clinical Trials. J. Clin. Oncol. *40*, 1474–1486. https://doi.org/10.1200/JCO.21.02377.
47. Sakaue, S., Kanai, M., Tanigawa, Y., Karjalainen, J., Kurki, M., Koshiba, S., Narita, A., Konuma, T., Yamamoto, K., Akiyama, M., et al. (2021). A cross-population atlas of genetic associations for 220 human phenotypes. Nat. Genet. *53*, 1415–1424. https://doi.org/10.1038/s41588-021-00931-x.
48. Kiuchi, Z., Nishibori, Y., Kutsuna, S., Kotani, M., Hada, I., Kimura, T., Fukutomi, T., Fukuhara, D., Ito-Nitta, N., Kudo, A., et al. (2019). GLCCI1 is a novel protector against glucocorticoid-induced apoptosis in T cells. Faseb. J. *33*, 7387–7402. https://doi.org/10.1096/fj.201800344RR.
49. Astle, W.J., Elding, H., Jiang, T., Allen, D., Ruklisa, D., Mann, A.L., Mead, D., Bouman, H., Riveros-Mckay, F., Kostadima, M.A., et al. (2016). The Allelic Landscape of Human Blood Cell Trait Variation and Links to Common Complex Disease. Cell *167*, 1415–1429.e19. https://doi.org/10.1016/j.cell.2016.10.042.
50. Vuckovic, D., Bao, E.L., Akbari, P., Lareau, C.A., Mousas, A., Jiang, T., Chen, M.H., Raffield, L.M., Tardaguila, M., Huffman, J.E., et al. (2020). The Polygenic and Monogenic Basis of Blood Traits and Diseases. Cell *182*, 1214–1231.e11. https://doi.org/10.1016/j.cell.2020.08.008.
51. Lv, H., Zhang, M., Shang, Z., Li, J., Zhang, S., Lian, D., and Zhang, R. (2017). Genome-wide haplotype association study identify the FGFR2 gene as a risk gene for acute myeloid leukemia. Oncotarget *8*, 7891–7899. https://doi.org/10.18632/oncotarget.13631.
52. Hernández, L., Terradas, M., Camps, J., Martín, M., Tusell, L., and Genescà, A. (2015). Aging and radiation: bad companions. Aging Cell *14*, 153–161. https://doi.org/10.1111/acel.12306.
53. Schuster, B., Ellmann, A., Mayo, T., Auer, J., Haas, M., Hecht, M., Fietkau, R., and Distel, L.V. (2018). Rate of individuals with clearly increased radiosensitivity rise with age both in healthy individuals and in cancer patients. BMC Geriatr. *18*, 105. https://doi.org/10.1186/s12877-018-0799-y.
54. Welsh, C.E., Miller, D.R., Manly, K.F., Wang, J., McMillan, L., Morahan, G., Mott, R., Iraqi, F.A., Threadgill, D.W., and de Villena, F.P.M. (2012). Status and access to the Collaborative Cross population. Mamm. Genome *23*, 706–712. https://doi.org/10.1007/s00335-012-9410-6.
55. Mao, J.H., Langley, S.A., Huang, Y., Hang, M., Bouchard, K.E., Celniker, S.E., Brown, J.B., Jansson, J.K., Karpen, G.H., and Snijders, A.M. (2015). Identification of genetic factors that modify motor performance and body weight using Collaborative Cross mice. Sci. Rep. *5*, 16247. https://doi.org/10.1038/srep16247.
56. Love, M.I., Huber, W., and Anders, S. (2014). Moderated estimation of fold change and dispersion for RNA-seq data with DESeq2. Genome Biol. *15*, 550. https://doi.org/10.1186/s13059-014-0550-8.
57. Michalski, J.M., Janss, A.J., Vezina, L.G., Smith, K.S., Billups, C.A., Burger, P.C., Embry, L.M., Cullen, P.L., Hardy, K.K., Pomeroy, S.L., et al. (2021). Children's Oncology Group Phase III Trial of Reduced-Dose and Reduced-Volume Radiotherapy With Chemotherapy for Newly Diagnosed Average-Risk Medulloblastoma. J. Clin. Oncol. *39*, 2685–2697. https://doi.org/10.1200/JCO.20.02730.

STAR★METHODS

KEY RESOURCES TABLE

REAGENT or RESOURCE	SOURCE	IDENTIFIER
Chemicals, peptides, and recombinant proteins		
PE Rat anti Mouse CD3 Molecular Complex	Becton Dickinson and Company	Cat# 555275; RRID:AB_395699
PerCP Rat anti Mouse CD45R/B220	Becton Dickinson and Company	Cat# 553093; RRID:AB_394622
APC Rat anti Mouse CD8a	Becton Dickinson and Company	Cat# 553035; RRID:AB_398527
Alexa Fluor 488 Rat anti Mouse CD4	Becton Dickinson and Company	Cat# 557667; RRID:AB_396779
MethoCult GF	StemCell Technologies	M3434
Critical commercial assays		
ApopTag Plus Peroxidase *in situ* Apoptosis kit	Sigma	S7101
Mouse RiboPUre Blood RNA Isolation kit	ThermoFisher Scientific	AM1951
Lineage Cell Depletion Kit, mouse	Miltenyi Biotec Inc	130-090-858
CS/2 FS-PAK^{TM} REAGENTS (For HemaVET 950FS)	Drew scientific	200106
Deposited data		
RNA sequencing data	This paper	NCBI SRA (PRJNA945475)
Experimental models: Organisms/strains		
Mouse: Collaborative Cross mice	Systems Genetics Core Facility University of North Carolina	CC001/Unc, CC002/Unc, CC003/Unc, CC004/Tau, CC005/TauUnc CC006/TauUnc CC008/GeniUnc, CC009/Unc, CC011/Unc, CC012/GeniUnc CC013/GeniUnc, CC015/Unc, CC016/GeniUnc, CC017/Unc, CC019/TauUnc, CC021/Unc, CC024/GeniUnc, CC026/GeniUnc, CC028/GeniUnc, CC030/GeniUnc, CC032/GeniUnc, CC033/GeniUnc, CC036/Unc, CC037/TauUnc, CC038/GeniUnc, CC039/Unc, CC040/TauUnc, CC041/TauUnc, CC042/GeniUnc, CC051/TauUnc, CC057/Unc, CC061/GeniUnc CC080/TauUnc CC081/Unc CC084/TauUnc
Software and algorithms		
SPSS	IBM	version 24

(*Continued on next page*)

Continued

REAGENT or RESOURCE	SOURCE	IDENTIFIER
R version	https://www.r-project.org/	Version 3.6.2
Other		
Novaseq SP	Ilumina	N/A

RESOURCE AVAILABILITY

Lead contact

Further information and requests for reagents and resources should be directed to and will be fulfilled by the lead contact, Antoine M. Snijders, Biological Systems and Engineering Division, Lawrence Berkeley National Laboratory (AMSnijders@lbl.gov).

Materials availability

This study did not generate new unique reagents.

Data and code availability

All data needed to evaluate the conclusions in the paper are presented in the paper and/or the Supplementary Materials. RNA-Seq data are available without restrictions from the Sequence Read Achieve (SRA) at the National Center for Biotechnology Information (NCBI) under BioProject accession (PRJNA945475).

EXPERIMENTAL MODEL AND SUBJECT DETAILS

CC mice experiments

All CC mice were purchased from the Systems Genetics Core Facility at The University of North Carolina at Chapel Hill.

METHOD DETAILS

Mice and radiation exposure

CC mice were obtained from the Systems Genetics Core Facility at The University of North Carolina (UNC) at Chapel Hill.[54] Mice were acclimated at LBNL for 8 weeks prior to the initiation of breeding as previously described.[55] The study was carried out in strict accordance with the Guide for the Care and Use of Laboratory Animals of the National Institutes of Health. The Animal Welfare and Research Committee at Lawrence Berkeley National Laboratory approved the animal use protocol. For each strain, 12-week old mice were exposed to 1 Gy or sham, using a Precision X-ray Inc XRAD320 320 kVp X-ray machine, operated at 300 kV, 2 mA (dose rate of 196 mGy/min). Dosimetry was performed using a RadCal ion chamber (Radcal 10X6-0.18). After radiation exposure, mice were returned to their cage and left undisturbed for either 24 h or 4 weeks, then euthanized for blood collection. All mouse irradiations were performed between 1 and 2p.m. and all blood collections were performed 24 h or 4 weeks after radiation exposure between 1 and 3p.m.

Mouse blood analysis

Whole blood was collected into EDTA-coated tubes (Fisher Scientific). A complete blood cell count was acquired using a HemaVet950FS and specific lymphocyte subpopulations were assessed by FACS with cell specific markers for B-cells, T-cells, T-helper and T-suppressor cells using the following antibodies (BD Biosciences): rat anti mouse CD3-PE; rat anti mouse CC45R/B220 PerCP; rat anti mouse CD8a antibody APC; rat anti mouse CD4 antibody Alexa 488. The percentages of cells in blood were determined using a BD FACS Calibur (Becton Dickinson) and data were analyzed with FlowJo software (Tree Star, Inc.). Absolute lymphocyte and lymphocyte subpopulations were calculated based on the HemaVet Lymphocyte counts and relative abundance of lymphocyte subpopulations based on the FACS data.

Isolation of mouse hematopoietic stem cells and granulocyte macrophage-colony forming unit (GM-CFU) assay

Male CC019 and CC042 were whole-body irradiated with 1 Gy X-rays (n = 12 per strain) or sham irradiated (n = 12 per strain) at 12 weeks of age and euthanized at 24 h or 4 weeks after sham (n = 6 per strain) or radiation (n = 6 per strain) exposure. Bilateral femurs were removed and for each strain, dose and timepoint three pools of two mice each were collected. A 26-gauge sterile needle was inserted into the bone marrow cavity, and marrow was extruded by flushing with 10 mL of buffer (a solution containing PBS (phosphate buffered saline) pH 7.2, 0.5% BSA (bovine serum albumin) and 2mM EDTA). Flushed bone marrow from individual femurs were pooled together and pipetted up and down to prepare a single cell suspension and passed through 40 μm nylon meshes (BD Biosciences, Sparks, MD, USA). Mouse bone marrow Lin^- cells were obtained using a cocktail of biotinylated antibodies against a panel of "lineage" antigens (CD5, CD45R (B220), CD11b, Anti-Gr-1 (Ly-6G/C), 7-4, and Ter-119 antibodies) and Anti-Biotin MicroBeads

(Miltenyi Biotec Inc., Auburn, CA, USA) following the manufacturer's instructions. Isolated Lin^- cells were counted using a cell counter (Beckman Coulter, Brea, CA, USA), and from each pool, 1×10^4 cells were plated in triplicate in ultra-low attachment 6-well plates (Corning, NY, USA) using methocult (M3434, StemCell Technologies). The plates were incubated at 37°C in 5% CO_2 and $\geq$95% humidity for 11 days, and colonies (G/M/GM: granulocyte and macrophage progenitors, BFU-E: burst forming unit erythroid and GEMM: granulocyte, erythrocyte, monocyte, megakaryocyte) were counted using a dissecting microscope (Leica, Wetzlar, Germany).

Apoptosis assay

Cell death of lineage negative cells was detected using the ApopTag Plus Peroxidase *in situ* apoptosis detection kit (S7101, Millipore, Billerica, MA, USA) according to manufacturer's instruction. Briefly, cell suspensions were fixed in 1% paraformaldehyde in PBS, pH 7.4 overnight at room temperature (3 coverslips for each group). The endogenous peroxidase activity was quenched using 3% hydrogen peroxide in PBS at room temperature. Following incubation with terminal deoxynucleotidyl transferase (TdT) at 37°C for 1 h, the apoptotic cells were visualized under a bright field microscope by a diaminobenzidine (DAB) based detection system supplied with the kit, and sections were counterstained using methyl green (Trevigen, Gaithersburg, MD, USA) nuclear stain. TUNEL positive cells were counted in 5 randomly chosen high power fields (63×, Oil) microscopic fields (n = 2 and 3 coverslips from each group were scored and used for statistical analysis).

Radiation resistance score

Based on the hypothesis that the immune-related phenotypes are more resistant in radio-resistant strains/animals compared with those in radio-sensitive strains/animals, the radiation resistance score was therefore defined at a specific timepoint for each irradiated animal as fitting deviation between the estimated probability (i.e., using logistic regression model) of irradiation status and the ground truth probability of irradiation (i.e., 1). Specifically, at a certain timepoint (i.e., 24 h or 4 weeks), the radiation resistance score was calculated as follows, 1) Phenotype normalization: Strain-specific normalization was performed for all phenotypes in irradiated animals as the ratio of each individual phenotype over the median phenotype in the control animals belonging to the same strain; 2) Phenotype selection: univariate and stepwise multivariate logistic regression were applied for the selection of phenotypes that significantly contributed to the differentiation of control and irradiated animals; 3) Bootstrapping estimation: Bootstrapping strategy with 10,000 iterations at sampling rate 0.6 was applied for radio-resistance scoring. During each iteration, 60% samples were randomly selected for logistic regression model construction based on preselected phenotypes (see step 2), and the rest 40% samples were used for independent testing (i.e., irradiation probability estimation and fitting deviation calculation). At last, the radiation resistance score was calculated as the median fitting deviation of each irradiated animal over all 10,000 iterations.

Genome-wide association analysis

Genotype data of 134,593 SNPs was obtained from the UNC Systems Genetics Core website (http://csbio.unc.edu/CCstatus/index.py). SNPs were filtered based on minor allele frequency $\geq$5 out of the 35 CC strains, leaving 83,282 SNPs. At each SNP, hematologic parameters and radiation resistance scores for all CC mice were assigned to their respective alleles. The Mann-Whitney U test was used to test the significance of associations between each parameter and allele classes at each SNP. Quantitative trait loci (QTLs) were defined as two or more SNPs with P-values of association below the threshold of significance whereby adjacent SNPs were less than 1.5 Mb apart. QTL boundaries were set at the SNP locations of the most proximal and most distal SNP within a QTL where all neighboring significant SNPs were less than 1.5 Mb from each other. Putative candidate genes were defined as those genes (gencode.vM741) located within the boundaries of significant SNPs for each QTL. Human GWAS data was downloaded on 11/08/2022 from https://www.ebi.ac.uk/gwas/.

RNA isolation and sequencing

Whole blood was collected from male and female mice from six CC strains. For each strain blood was pooled from two male and two female mice, separately. Total whole blood RNA was isolated from 12-week-old mice using the Qiagen Mouse RiboPure Blood RNA Isolation Kit (Invitrogen). RNA quality was assessed using a BioAnalyzer (RIN values ranged from 8.3 to 9.6). Sequencing was performed at the UCLA Technology Center for Genomics & Bioinformatics on an Illumina Novaseq platform, generating 150bp paired end reads. RNA-Seq data has been deposited at NCBI SRA under accession code PRJNA945475. RNA-sequencing reads were mapped to the mouse genome (GRCm38/mm10 reference) using align function in Rsubread package (version 2.0.1) with default parameters. For each replicate, per-gene counts of uniquely mapped reads were computed using featureCounts function in Rsubread package (version 2.0.1). Differential expression analysis was performed and normalized gene counts were generated using DESeq2 v1.16.1.[56] The significance of overlap between candidate genes identified by RNA-sequencing and QTL analysis was calculated based on the hypergeometric distribution and the representation factor by calculating the number of overlapping genes divided by the expected number of overlapping genes drawn from two independent groups.

Radiation resistance score transfer from mouse to human

Following the definition of radiation resistance score above, a multivariate logistic regression model was first established based on pre-selected phenotypes (i.e., univariate and stepwise multivariate selection after normalization) from all common phenotypes

between mouse and human cohorts; and then directly applied to human cohort for the calculation of radiation resistance score in each individual human patient.

Medulloblastoma patient cohort

The Human Subjects Committee at Lawrence Berkeley National Laboratory approved the protocol for the analyses of blood count data obtained from medulloblastoma patients. Patients with medulloblastoma were treated with 1.8 Gy daily fractions for a total dose of 54–55.8 Gy. The total dose after the first week of treatment in our medulloblastoma cohort was 9 Gy in 5 fractions. Blood count data were obtained before the start of radiotherapy and one week after the first week of treatment. Most medulloblastoma patients (n = 90) received concurrent vincristine treatment as per Children's Oncology Group Protocol ACNS0331 and thus, received their first dose of vincristine during the 2 nd week of radiation.[57] Thus, vincristine did not affect the baseline or first complete blood count after RT in our cohort.

QUANTIFICATION AND STATISTICAL ANALYSIS

All statistical analysis were performed in R (version 3.6.2) and IBM SPSS (version 24). The Mann-Whitney U test was used to test the significance of associations between each parameter and allele classes at each SNP; as well as between each parameter and treatment groups. Spearman's rank correlation was used to evaluate the correlation among parameters. P-value<0.05 was considered statistically significant.